

UNCLASSIFIED

AD NUMBER

AD856845

LIMITATION CHANGES

TO:

Approved for public release; distribution is unlimited.

FROM:

**Distribution authorized to U.S. Gov't. agencies and their contractors;
Administrative/Operational Use; 30 JUN 1969.
Other requests shall be referred to Army Aviation Materiel Labs., Fort Eustis, VA.**

AUTHORITY

USAAMRDL ltr, 23 Jun 1971

THIS PAGE IS UNCLASSIFIED

AD856845

Solar RDR-1625-4
1
(2)

QUARTERLY TECHNICAL PROGRESS REPORT No. 4
1 April through 30 June 1969
MECHANISMS OF SAND AND DUST EROSION
IN GAS TURBINE ENGINES

By

C. E. Smeltzer

M. E. Gulden

W. A. Compton

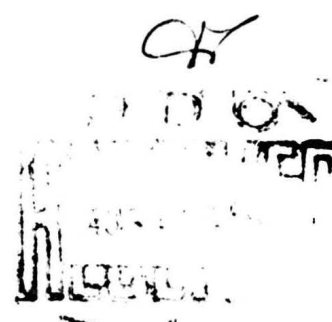
Prepared by

Solar Division of International Harvester Company
San Diego, California

~~STATEMENT OF INFORMATION~~

This document is subject to special export control regulations.
For transmission to foreign governments or foreign nationals,
made only with prior approval of ~~the U.S. Government~~
U. S. Army Aviation Materiel Laboratories
Fort Eustis, Virginia

Contract DAAJ02-68-C-0056



**BLANK PAGES
IN THIS
DOCUMENT
WERE NOT
FILMED**

DISCLAIMERS

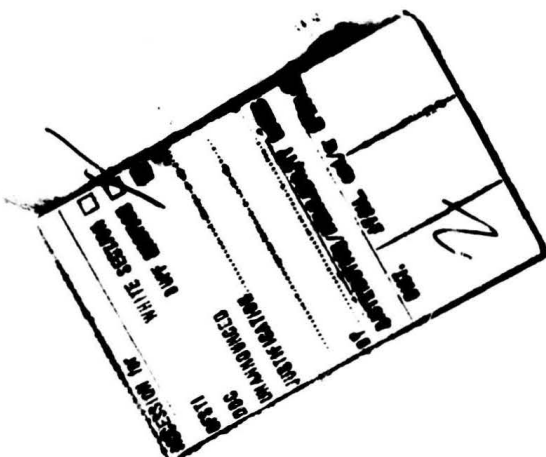
The findings in this report are not to be construed as an official Department of the Army position unless so designated by other authorized documents.

When Government drawings, specifications, or other data are used for any purpose other than in connection with a definitely related Government procurement operation, the United States Government thereby incurs no responsibility nor any obligation whatsoever; and the fact that the said drawings, specifications, or other data is not to be regarded by implication or otherwise as in any manner licensing the holder or any other person or corporation, or conveying any rights or permission, to manufacture, use, or sell any patented invention that may in any way be related thereto.

DISPOSITION INSTRUCTIONS

Destroy this report when no longer needed. Do not return it to originator.

This document may not be reproduced or published in any form in whole or in part without prior approval of the Government. Since this is a progress report, the information herein is tentative and subject to changes, corrections, and modifications.



DDC AVAILABILITY NOTICES

1. This document has been approved for public release and sale; its distribution is unlimited.
2. This document is subject to special export controls, and each transmittal to foreign governments or foreign nationals may be made only with prior approval of US Army Aviation Materiel Laboratories, Fort Eustis, Virginia 23604.
3. In addition to security requirements which must be met, this document is subject to special export controls and each transmittal to foreign governments or foreign nationals may be made only with prior approval of US Army Aviation Materiel Laboratories, Fort Eustis, Virginia 23604.
4. Each transmittal of this document outside the agencies of the US Government must have prior approval of US Army Aviation Materiel Laboratories, Fort Eustis, Virginia 23604.
5. In addition to security requirements which apply to this document and must be met, each transmittal outside the agencies of the US Government must have prior approval of US Army Aviation Materiel Laboratories, Fort Eustis, Virginia 23604.
6. Each transmittal of this document outside the Department of Defense must have prior approval of US Army Aviation Materiel Laboratories, Fort Eustis, Virginia 23604.
7. In addition to security requirements which apply to this document and must be met, each transmittal outside the Department of Defense must have prior approval of US Army Aviation Materiel Laboratories, Fort Eustis, Virginia 23604.
8. This document may be further distributed by any holder only with specific prior approval of US Army Aviation Materiel Laboratories, Fort Eustis, Virginia 23604.
9. In addition to security requirements which apply to this document and must be met, it may be further distributed by the holder only with specific prior approval of US Army Aviation Materiel Laboratories, Fort Eustis, Virginia 23604.

DISCLAIMER

10. The findings in this report are not to be construed as an official Department of the Army position unless so designated by other authorized documents.
11. When Government drawings, specifications, or other data are used for any purpose other than in connection with a definitely related Government procurement operation, the United States Government thereby incurs no responsibility nor any obligation whatsoever; and the fact that the Government may

have formulated, furnished, or in any way supplied the said drawings, specifications, or other data is not to be regarded by implication or otherwise as in any manner licensing the holder or any other person or corporation, or conveying any rights or permission, to manufacture, use, or sell any patented invention that may in any way be related thereto.

12 Trade names cited in this report do not constitute an official endorsement or approval of the use of such commercial hardware or software.

DISPOSITION INSTRUCTIONS

13. Destroy this report when no longer needed. Do not return it to the originator.

14. When this report is no longer needed, Department of the Army organizations will destroy it in accordance with the procedures given in AR 380-5.

AD856845

Contract DAAJ02-68-C-0056

1 April Through 30 June 1969

QUARTERLY TECHNICAL PROGRESS REPORT NO. 4

Solar R. P. 2-2752-7

**MECHANISMS OF SAND AND DUST EROSION IN
GAS TURBINE ENGINES**

By

**C. E. Smeltzer
M. E. Gulden
W. A. Compton**

**Solar Division of International Harvester Company
San Diego, California**

For

**U. S. Army Aviation Materiel Laboratories
Fort Eustis, Virginia**

ABSTRACT

Dust erosion damage of military gas turbines is a serious problem in many current service areas. The subject program is designed to gain an improved understanding of the various mechanisms of dust erosion, as a basis for possible future development of turbine materials with improved innate erosion resistance. A materials science approach to the problem is emphasized, to observe, measure, and study erosion phenomena at the target surface. The object is to define working physical and mathematical models of the erosion processes, from consideration of both erosion data and phenomenological information gathered.

The experimental program is organized to evaluate the relative importance of erosion influencing variables introduced by the carrier gas, the dust suspension and the target materials themselves. Test conditions have been chosen to simulate the range of gas temperatures (RT - 800 F) static pressures (1 - 16 atmospheres) and gas and particle velocities (500-1500 fps) encountered in a typical high-performance compressor. High velocity dust suspensions are programmed to impinge upon standard target specimens (stressed from 0-60% of the yield stress), representing current and advanced candidate materials for compressor blading. Dust varieties representative of both American and Southeast Asia theaters of operation have been scheduled. Erosion rate and erosion factor are to be measured and evaluated as functions of impingement angle, heat treat condition of target, dust particle size, mass, energy and concentration as well as previously cited variables. The data is to be analyzed statistically to determine the principal control variables and their significant interactions. Erosion phenomena will be studied using conventional metallographic techniques and scanning electron microscopy.

The program is divided into five functional tasks; viz. (1) a literature survey and data review, (2) an analysis of the physical environment in a typical high-performance compressor and the formulation of an erosion test program based on this environment, (3) the execution of the erosion test program, including the design and construction of special test equipment, (4) the analysis of erosion data and development of physical and mathematical models to define erosion mechanisms, and (5) organization of the erosion data in forms useful to the design engineer and the materials development specialist. Tasks III, IV and V are reported upon this period.

FOREWORD

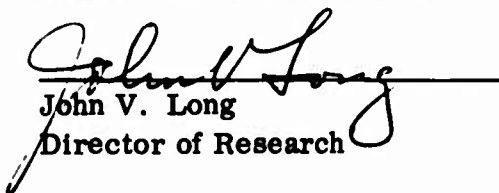
This is the fourth quarterly technical progress report covering work done under Contract No. DAAJ02-68-C-0056 during the period 1 April to 30 June 1969. The program is being conducted under the direction of Mr. David B. Cale, representative of the Contracting Officer, U. S. Army Aviation Materiel Laboratories, Fort Eustis, Virginia. The program work is being conducted by the Research Laboratory of the Solar Division of International Harvester Company under the cognizance of C. E. Smeltzer, Principal Investigator, and W. A. Compton, Program Manager. Acknowledgement is given to H. Mnew of Solar for engineering analysis of particle acceleration characteristics and compressor environment studies and to Professor I. Finnie of the University of California, for consultation in the review of literature and experimental program design. (Mrs.) M. E. Gulden of Solar has conducted the electron microscopy studies of erosion surfaces. M. A. Gould and F. Crinion of Solar have assisted in the development of experimental techniques and equipment. Dr. G. E. Bowie of Solar has assisted in the analysis of erosion data and construction of nomographs (Series III).

PUBLICATION REVIEW

Approved:



W. A. Compton
Asst. Director of Research



John V. Long
Director of Research

CONTENTS

Section		Page
1	INTRODUCTION	1
2	PROGRAM PLAN AND OBJECTIVES	3
3	OUTLINE OF PROGRAM TASKS	5
4	RESULTS AND DISCUSSION	7
	4.1 THE EROSION TEST PROGRAM (TASK III)	7
5	SYNOPSIS OF PROGRAM STATUS	53
6	REFERENCES	55
	Appendix A	
	Appendix B	

ILLUSTRATIONS

Figure		Page
1	Volume Erosion Factor (ϵ_V) Versus Single Particle Volume (Δ)	10
2-9	Average Target Volume Loss Per Single Particle Impact (E_V) Versus Single Particle Volume (Δ)	11-18
10	Average Target Volume Loss Per Single Particle Impact (E_V) Versus Particle Velocity (V)	19
11-18	Average Target Volume Loss Per Single Particle Impact (E_V) Versus ΔV^2	37-44
19	Plots of E_V Versus ΔV^2 for all Target Material and Impingement Angle Combinations	46
20	Nomograph Relating Δ, V, and E_V for the Ti-6Al-4V Target (A.R. Dust; 37.5° Impingement Angle)	47

TABLES

Table		Page
1	Series III Test Format (Part I) Arizona Road Dust Subseries	8
2	Compilation of Series III Test Data (Part I; 2024 Al Target)	20
3	Compilation of Series III Test Data (Part I; Ti-6Al-4V Target)	24
4	Compilation of Series III Test Data (Part I; 410 SS Target)	28
5	Compilation of Series III Test Data (Part I; 17-7 PH Target)	32

I. INTRODUCTION

The modern gas turbine engine with excellent power to weight performance has proven a valuable asset in many military applications. However, since the gas turbine must use two or more times the air per horsepower than internal combustion engines, it becomes vulnerable to power degradation from entrained particles in the ingested air, such as dust and sand. Dust erosion of precision air foil sections in a compressor may destroy performance of a gas turbine in a very short period of time. Military publications admit that the replacement rate of gas turbines in the Southeast Asia Operations, as a result of dust erosion, currently amounts to about \$150,000,000 a year. Following an inspection tour of this area, a House Armed Services Sub-Committee of the U. S. Congress reported that engine life had been cut from a normal range of 1000 to 1600 hours to only 300 hours because of dust ingestion. Two approaches may be used to combat this problem. One is to develop a filtration system that will remove most of the solid particles from the main air stream and alleviate the erosion problem. The other is to design materials that are not appreciably affected by solid particle erosion and thus extend the engine life. Quite obviously, some compromise is necessary where advancements are made in both areas.

Dust filters and separators invariably decrease engine efficiency and require constant maintenance. Therefore, the optimum solution would appear to be new compressor materials with significantly improved innate erosion resistance. The proper design of these materials will require better understanding of the basic mechanisms of dust erosion and detailed characterization of the critical material properties and environmental conditions which influence erosion.

II. PROGRAM PLAN AND OBJECTIVES

The proposed program is designed to increase the present knowledge of dust erosion mechanisms on typical compressor materials in gas turbine environments. A materials science approach will be the basic one adopted. Emphasis is placed on the experimental phases of the program, with particular control over dust particle varieties, sizes, shapes, and concentrations as encountered in both American desert and Southeast Asian theaters of service. Environmental variables will be extended significantly also to more closely simulate actual engine conditions of high (near sonic) gas velocities, up to 1500 fps, high gas temperature (to 800 F) and high pressures (to 16 atmospheres). Target materials will be chosen to include typical current candidates for compressor blading (viz., 12-Cr and precipitation hardening stainless steels, high strength aluminum and titanium alloys and a composite material). The capability to stress the target specimen will be provided.

The principal objective of the program is to identify and then define the various mechanisms of erosion associated with high velocity dust particles striking a target. Both a physical and a mathematical model of each mechanism will be sought. Provided these mechanisms can be defined adequately, nomographs incorporating the controlling variables will be constructed to enable the design engineer to predict erosion performance of candidate engine materials. The secondary objective of the program is to provide the necessary guidelines for material developers to tailor new engineering materials that are especially resistant to sand and dust erosion.

A detailed test plan format was developed and is included in this report as Appendix A.

III. OUTLINE OF PROGRAM TASKS

The program will be carried out in five separate but interrelated tasks:

- Task I will include a comprehensive literature search condensing all information relevant to the study program. This search will include data on erosion rates of materials as affected by particle size, composition, and concentration in turbine field studies as well as under controlled laboratory conditions.
- Task II will include an analysis of the flow rates, velocities, pressures, temperatures, and incident angles in a typical turbine engine and V/STOL type air foil sections. This analysis will be more a documentation of trends and parameters used in preliminary analysis by gas turbine designers, allowing direct correlation with the results from the experimental program to various areas in the engine. An experimental erosion program will be formulated compatible with this analysis.
- Task III constitutes the experimental program which is organized to study the effects of particle size, concentration, velocity, angle, and composition on at least four target materials typical of gas turbine compressors. Other factors such as applied stress, static pressure, and temperature will be included in the program. (See Appendix A.)
- Task IV includes an analytical and theoretical study of the data generated in Task III, designed to define the mechanisms of erosion. Included in this study will be micrographs, from the newly developed scanning electron microscope, of target materials exposed to different particle size, concentration, and velocities in an attempt to define the basic interaction of dust particle with substrate. Professor Iain Finnie of the University of California, Berkeley, will act as a consultant to aid in the theoretical studies to evolve an analytical model that will better predict the mechanism of dust and sand erosion.

- Task V will include the organization of the data in a practical form that will be usable by the design engineer for predicting performance of gas turbine materials in dust environments. This task will pay particular attention to particle size, mass, particle concentration, and particle energy and velocity as they influence erosion rate, all as a function of impingement angle and target material.

Work this period has concentrated upon Tasks III and IV of the program plan.

IV. RESULTS AND DISCUSSION

4.1 THE EROSION TEST PROGRAM (TASK III)

Experiments this quarter were concentrated upon Test Series III of Task III (see Appendix A). All erosion tests were conducted using the erosion test facility described in the Second Quarterly Report (Ref. 1). Important subtasks reported here are:

- Outlining the Test Plan Format for Remainder of Test Series III
- Preparation of Vietnamese Laterite as a Test Dust
- Definition of the Dust Concentration Parameter

4.1.1 Data Presentation and Discussion; Test Series III

Test Series III is designed to determine the influence of varying test particle mass, M (or particle volume, Δ , for the same dust variety), particle velocity, V, and particle kinetic energy ($\propto \Delta V^2$) upon erosion. Target losses are measured and compared in terms of:

$$\epsilon \text{ (Weight Erosion Factor)} = \text{erosion weight loss (mgs) per gram of dust impacted}$$

$$\epsilon_V \text{ (Volume Erosion Factor)} = \text{erosion volume loss (cm}^3 \times 10^{-3}\text{) per gram of dust impacted}$$

$$E \text{ (Single Particle Parameter; Weight)} = \text{average target weight loss per single particle impact (mgs} \times 10^{-8}\text{)}$$

$$E \text{ (Single Particle Parameter; Volume)} = \text{average target volume loss per single particle impact (cm}^3 \times 10^{-11}\text{)}$$

A total of approximately 200 erosion tests have been conducted this quarter, following the test plan outlined in Table I. Duplicate room temperature tests were carried out for each condition, employing Arizona Road Dust in four different particle size fractions (viz., 0-43 μ , 43-74 μ , 74-147 μ , and 147-208 μ). Assuming the nearly

TABLE I
SERIES III TEST FORMAT (PART I)
ARIZONA ROAD DUST SUBSERIES ($\angle = 37.5$ and 60° ; $N = 5.40$ gms)

Temperature (° F)	Particle Size (μ)	Range, Estimated Particle Velocity (fps)	Particle Velocity, Median Particle Size (fps)	Carrier Gas (Air) Velocity (fps)	Test Time (sec)	P_T (in. Hg.)
RT	0-43	475/500	488	500	785	4.5
		650/685	670	685	570	9.3
		900/950	925	950	410	21.0
	43-74	475/500	488	525	745	5.2
		650/690	670	725	540	10.5
		900/950	880	950	410	21.0
	74-147	475/500	488	570	685	6.0
		650/690	670	760	515	12.0
		795/865	830	950	410	21.0
	147-208	475/500	488	605	645	7.0
		650/695	670	835	470	15.2
		715/795	755	950	410	21.0

equi-axed dust grains (predominantly silica quartz) are actually cubic particles, the single-particle volumes (Δ) for median-size particles in each fraction are $8.0 \times 10^{-9} \text{ cm}^3$, $1.9 \times 10^{-7} \text{ cm}^3$, $1.3 \times 10^{-6} \text{ cm}^3$, and $5.4 \times 10^{-6} \text{ cm}^3$, respectively. It was found that the Giannini powder feeder could not successfully meter the $0-43\mu$ dust fraction, due to caking and clogging problems. Consequently, a new gravity-feed dust meter was designed and constructed at Solar to handle all the fine and coarse dust fractions required in this and subsequent test series. The construction and operation of the new dust feeder are described in Appendix B.

The original intent was to test all dust fractions at three different particle velocities; viz., 488, 670, and 925 fps. The two lower velocities were attained with little difficulty. However, it was determined experimentally that the high carrier gas velocities (1000-1060 fps) required to accelerate all but the finest dust fraction to 925 fps were not attainable in the 10 foot by 1/4 inch diameter acceleration nozzle because of choking effects. A compromise solution adopted was to test all fractions at the highest carrier gas velocity attainable (viz., 950 fps), see Table I.

The weight of dust impacted per test was held constant at 5.40 grams, as in previous test series. The concentration of dust in the carrier gas (nozzle region) was maintained at a constant concentration of 40 mg/ft³. Details of the test procedure have been described in References 1 and 2.

Erosion test results have been tabulated for all four target materials (2024 aluminum alloy, Table II; Ti-6Al-4V alloy, Table III; 410 stainless steel, Table IV; and 17-7 PH stainless steel, Table V). The first plots made were of volume erosion factor (ϵ_V) versus median-particle volume (Δ), typified by Figure 1 for the titanium alloy target. These curves show very little variation in erosion factor, even though single particle volume, Δ , varies by three orders of magnitude. A much more sensitive parameter was found to be E_V , the average target volume loss per single particle impact. Log-log plots of E_V versus Δ yielded essentially straight-line relationships for almost every target material and particle velocity combination tested (see Fig. 2 through 9). The slopes of the curves for all velocities proved to be 1.0 ± 0.1 , suggesting a general equation of the type

$$E_V = C_0 \Delta^{(1.0 \pm 0.1)} \quad (1)$$

This proportional erosion volume- (and mass) to-particle volume (and mass) relationship is reasonable, inasmuch as the integral unit of the erosion mechanism is the impact of a single particle with the target, which (on the basis of statistical averaging) generates a predictable volume of erosion product, E_V . A more basic equation which considers the kinetic energy of the particle (for mechanism activation) is

$$E_V = KMV^m = K\rho\Delta^n V^m = CV^{2.0} \quad (2)$$

when n is assumed to be 1.0 and m is 2.0; and where

C_0 = system constant, equation (1) ($C_0 = K\rho V^{2.0}$)

C = system constant, equation (2) ($C = K\rho\Delta$)

M = median particle mass ($M = \rho\Delta$)

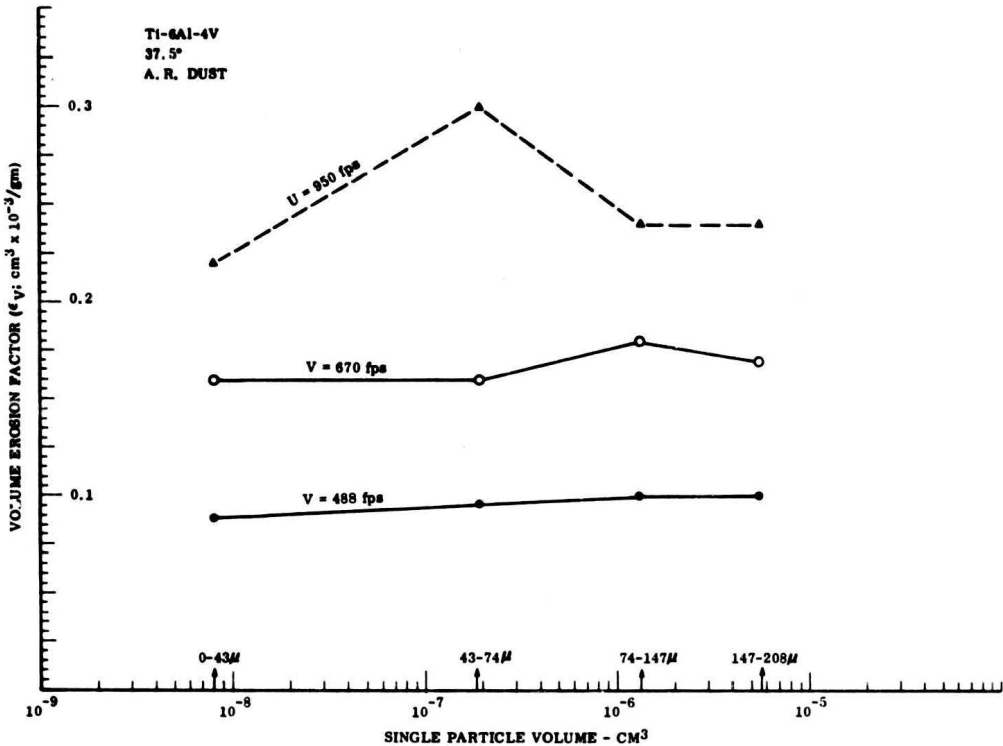


FIGURE 1. VOLUME EROSION FACTOR (ϵ_V) VERSUS SINGLE PARTICLE VOLUME (Δ)

ρ = dust particle density

K = basic system constant, equation (2) ($K = C/M$)

As an initial test of the validity of the energy-based equation (2), plots were drawn of ϵ_V versus V (particle velocity), and then analyzed as follows (using the Ti-6Al-4V target and 37.5 degree impingement angle as a typical example, Figure 10).

2024-Al (ANNEALED)
37.5°
A. R. DUST

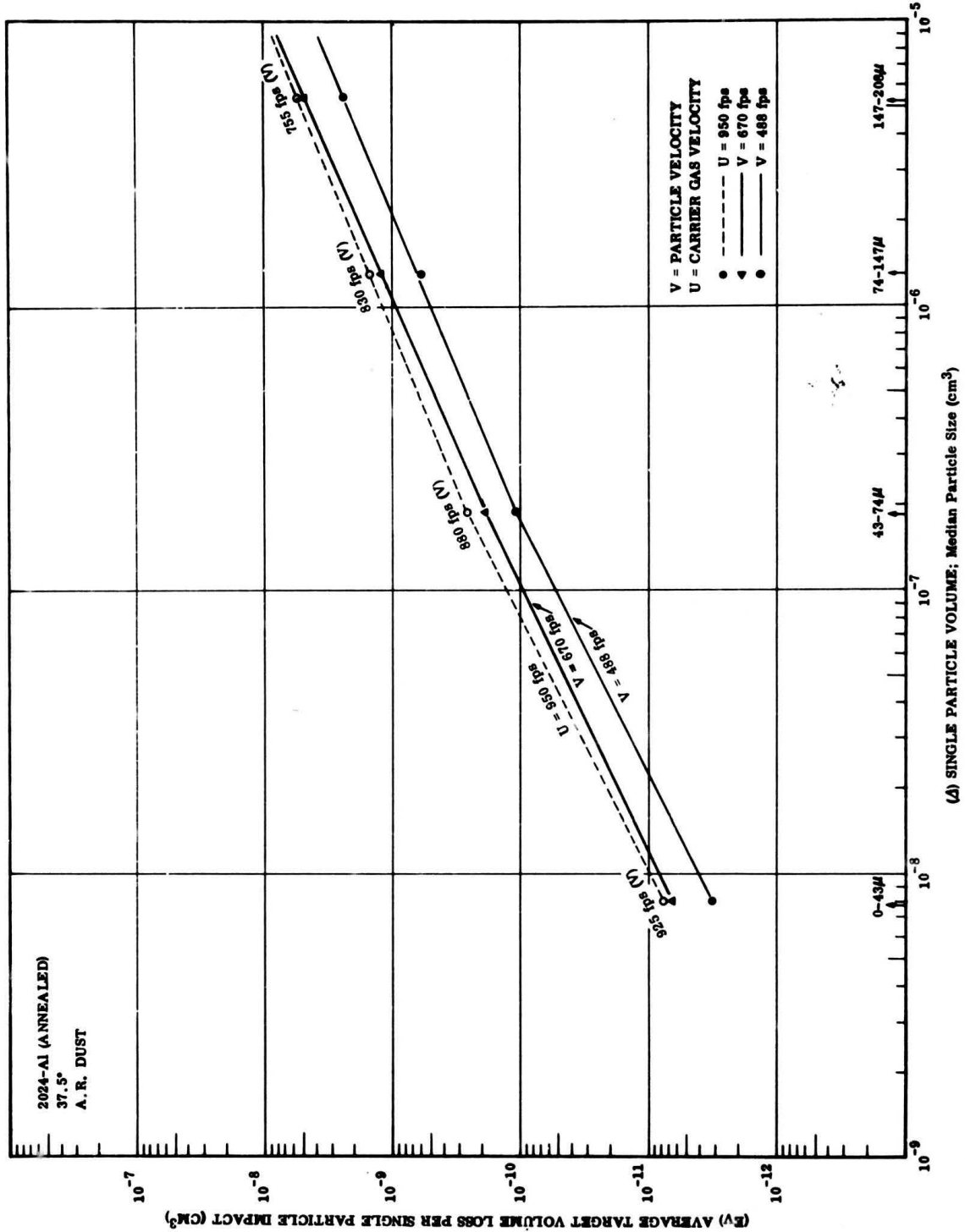


FIGURE 2 . AVERAGE TARGET VOLUME LOSS PER SINGLE PARTICLE IMPACT
(E_V) VERSUS SINGLE PARTICLE VOLUME (Δ)

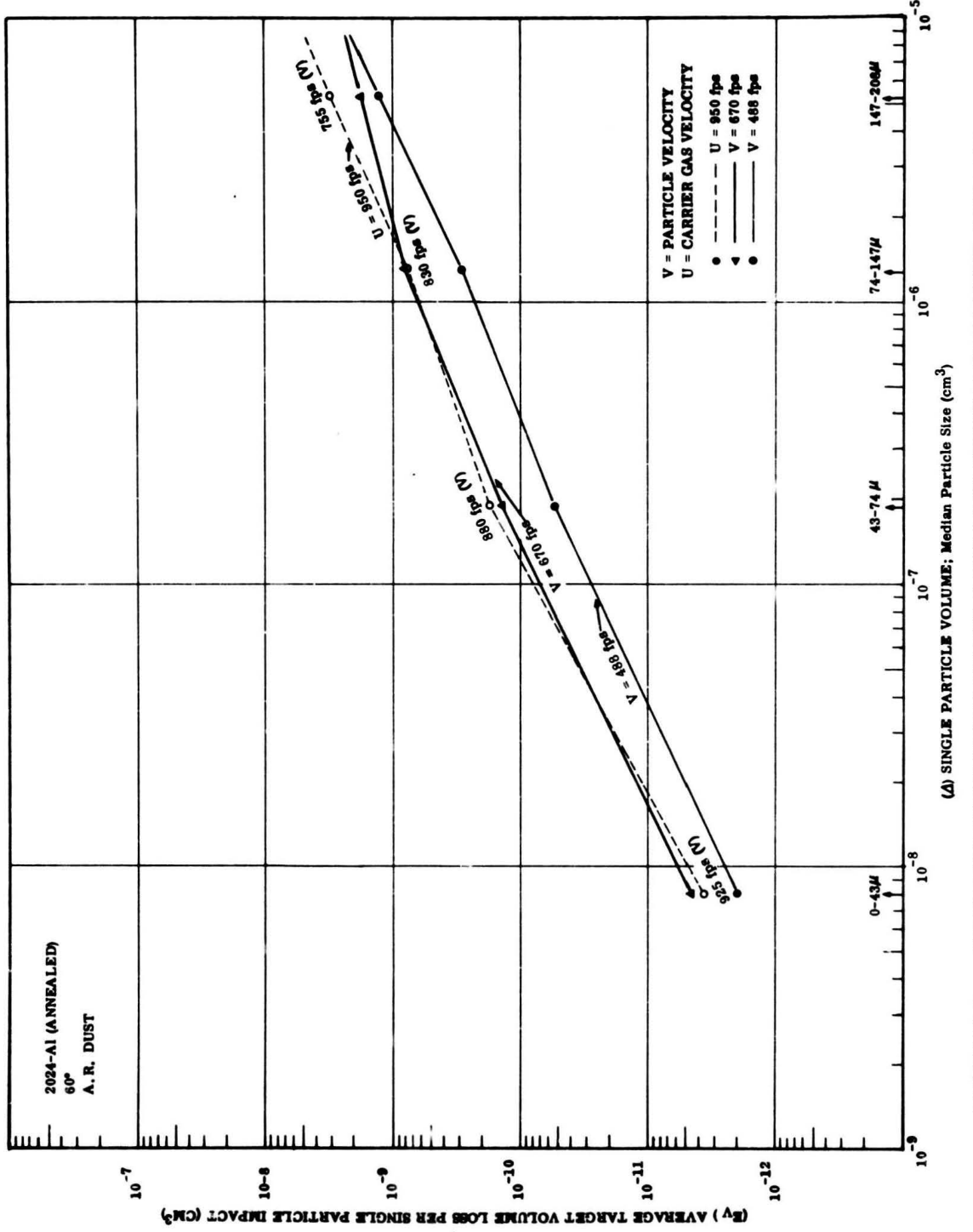


FIGURE 3. AVERAGE TARGET VOLUME LOSS PER SINGLE PARTICLE IMPACT
 (ΔV) VERSUS SINGLE PARTICLE VOLUME (Δ)

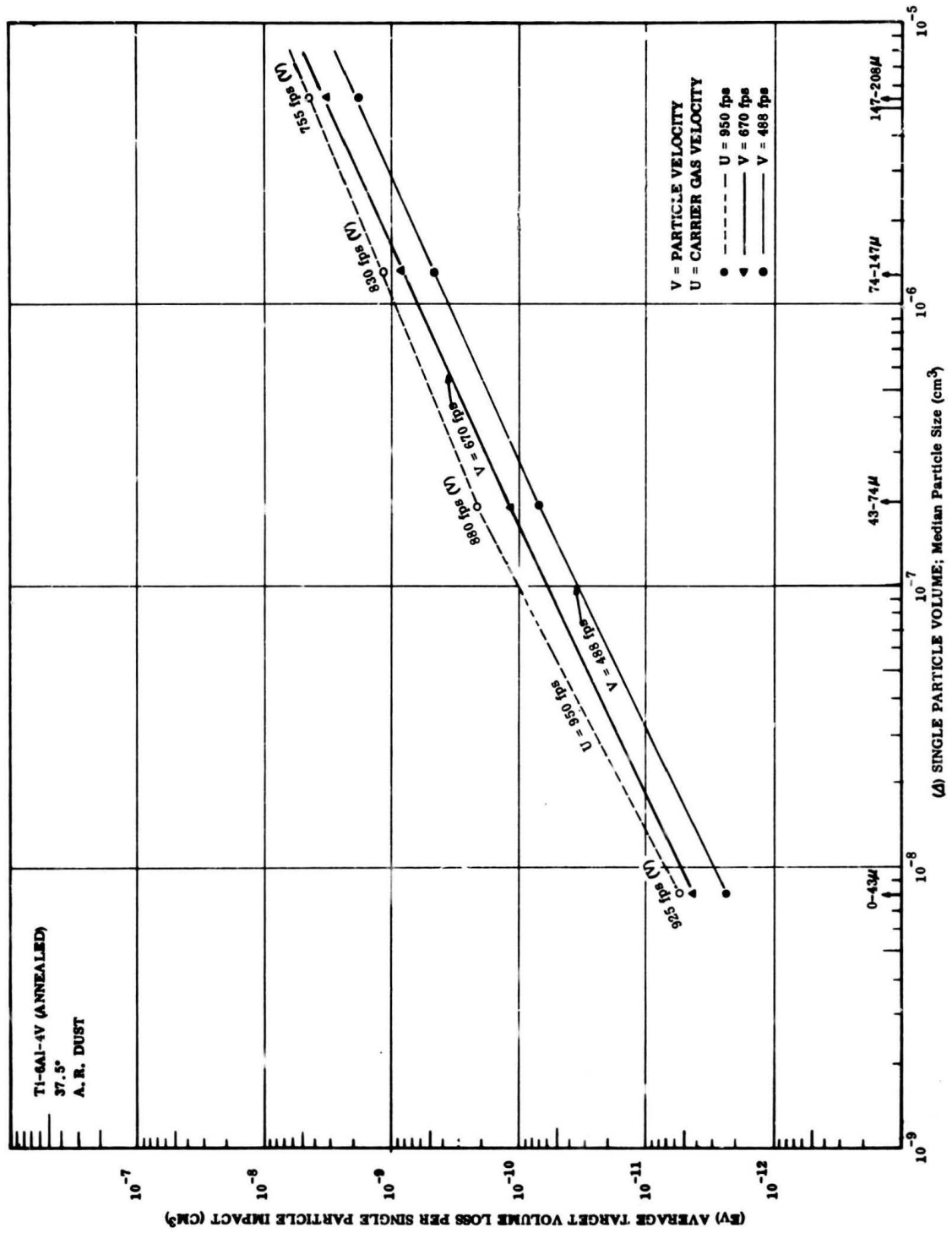


FIGURE 4. AVERAGE TARGET VOLUME LOSS PER SINGLE PARTICLE IMPACT
(EV) VERSUS SINGLE PARTICLE VOLUME (L)

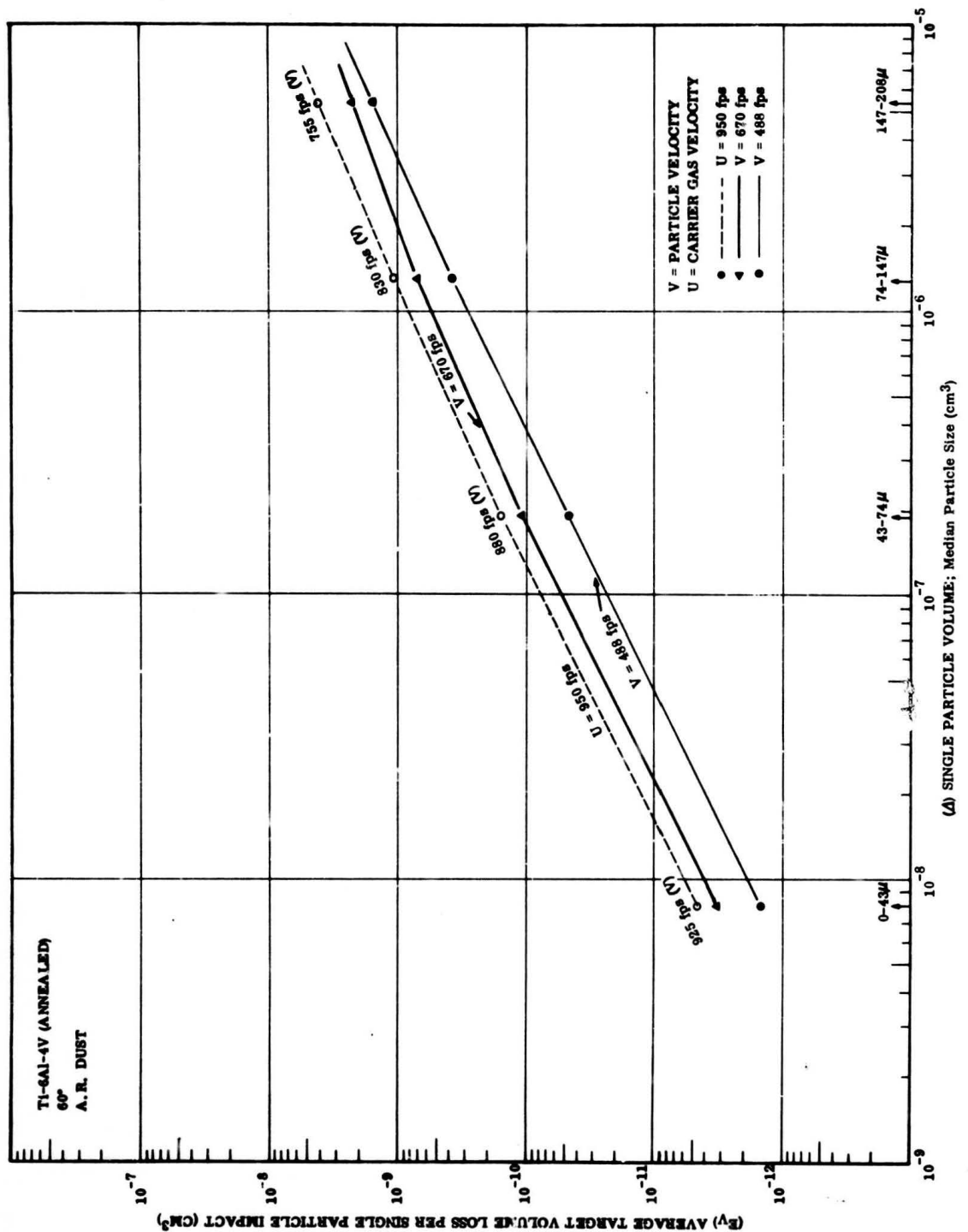


FIGURE 5. AVERAGE TARGET VOLUME LOSS PER SINGLE PARTICLE IMPACT
(E_V) VERSUS SINGLE PARTICLE VOLUME (Δ)

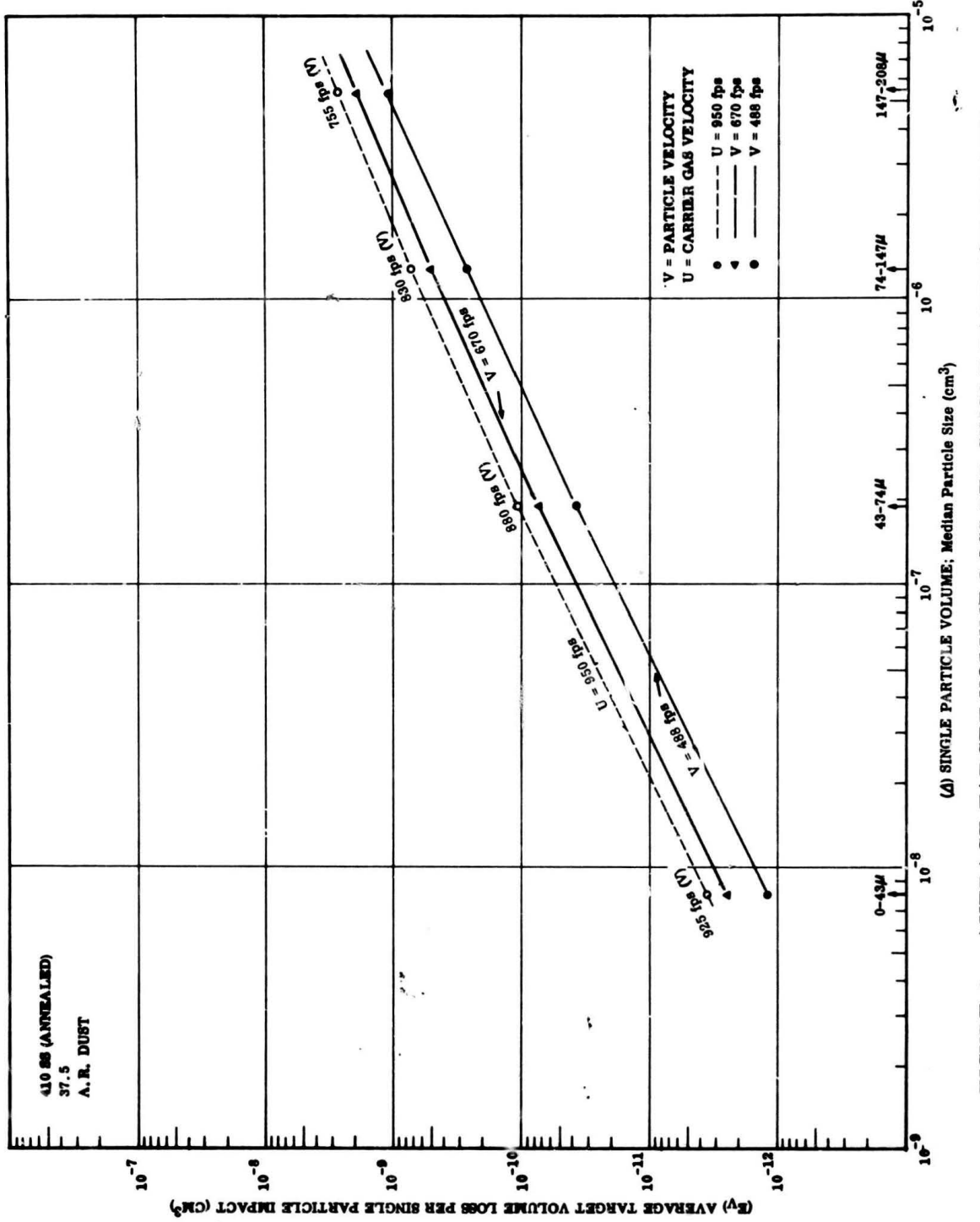


FIGURE 6. AVERAGE TARGET VOLUME LOSS PER SINGLE PARTICLE IMPACT
 (E_V) VERSUS SINGLE PARTICLE VOLUME (Δ)

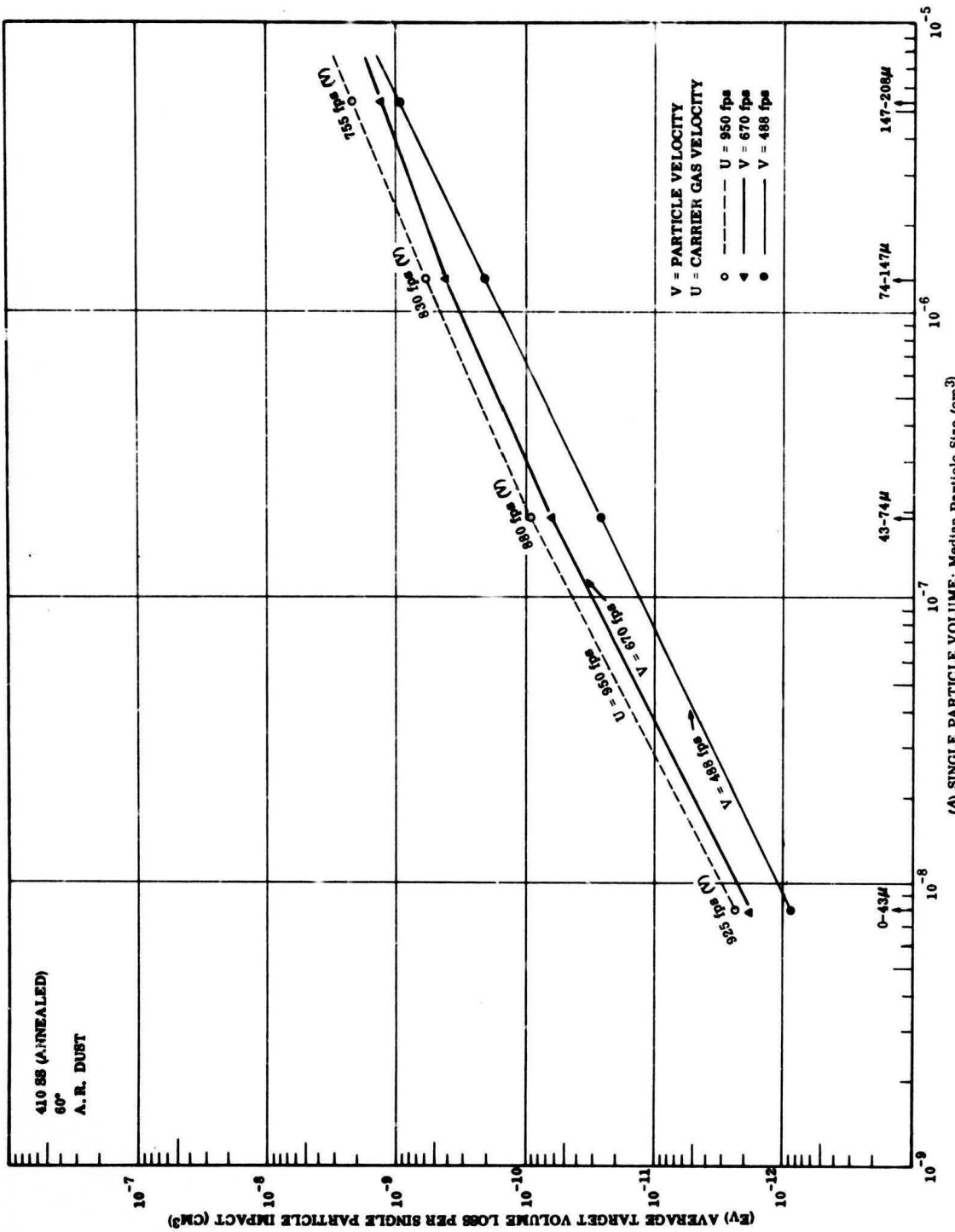


FIGURE 7. AVERAGE TARGET VOLUME LOSS PER SINGLE PARTICLE IMPACT
(ΔV) VERSUS SINGLE PARTICLE VOLUME (Δ)

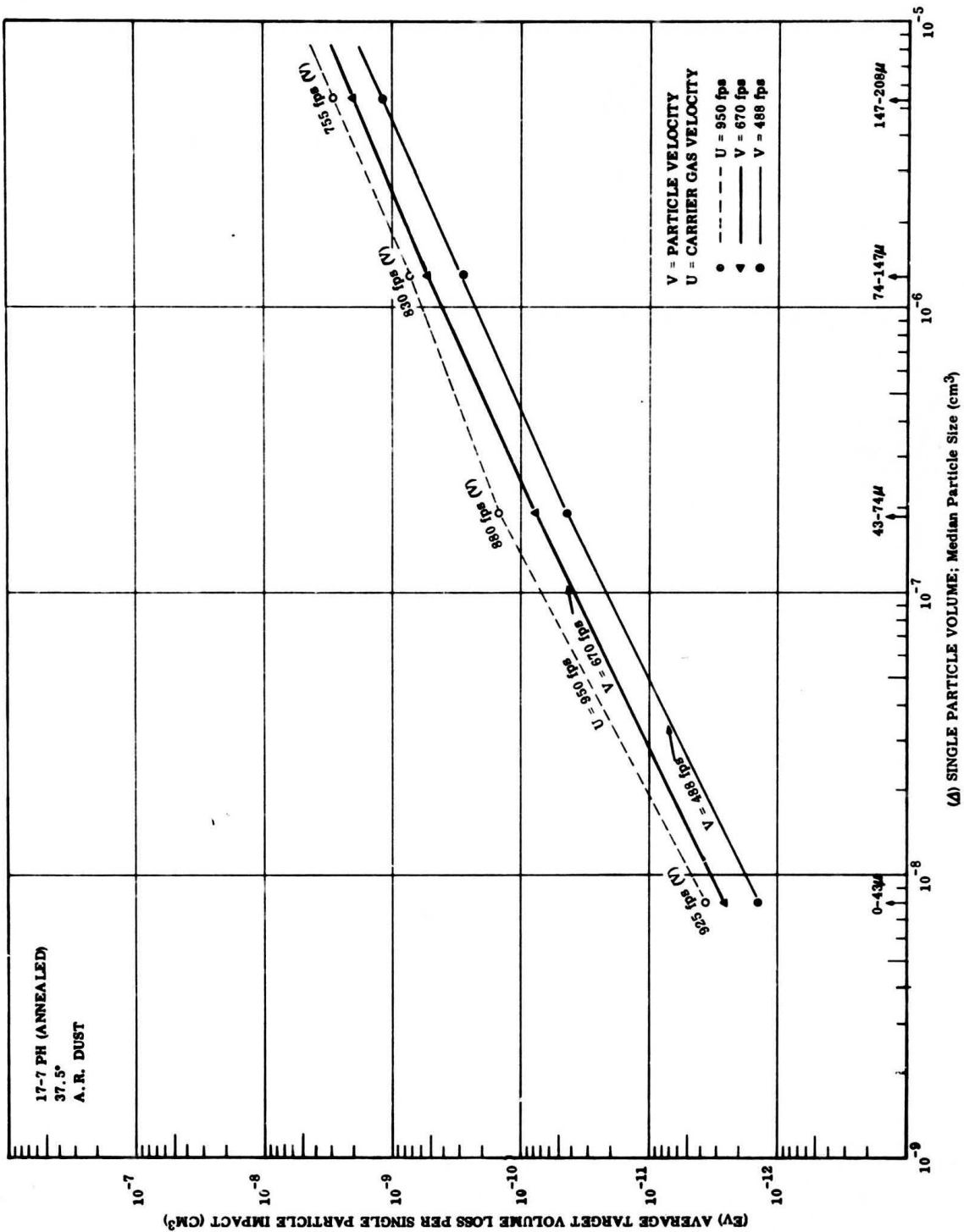


FIGURE 8. AVERAGE TARGET VOLUME LOSS PER SINGLE PARTICLE IMPACT
(EV) VERSUS SINGLE PARTICLE VOLUME (Δ)

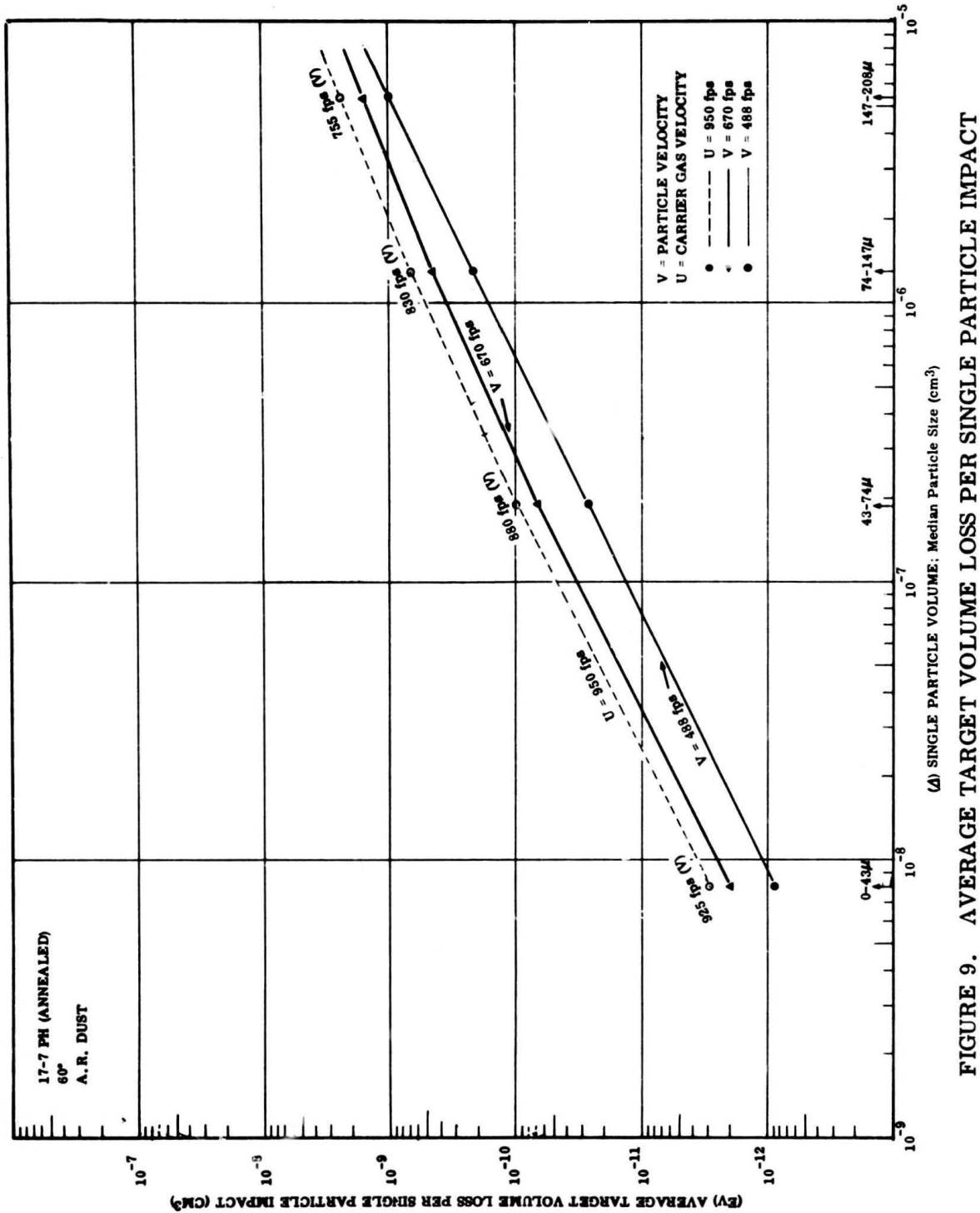


FIGURE 9. AVERAGE TARGET VOLUME LOSS PER SINGLE PARTICLE IMPACT (E_V) VERSUS SINGLE PARTICLE VOLUME (D)

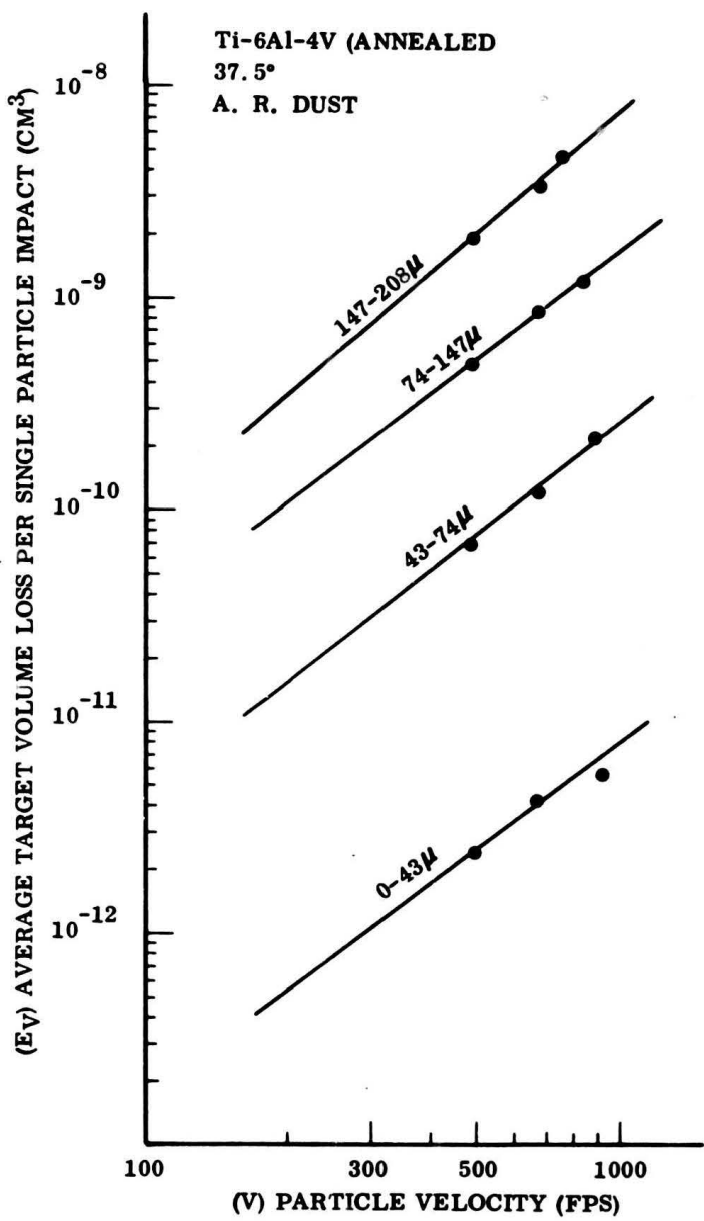


FIGURE 10. AVERAGE TARGET VOLUME LOSS PER SINGLE PARTICLE IMPACT (EV) VERSUS PARTICLE VELOCITY (V)

TABLE IIA

COMPIRATION OF SERIES III TEST DATA (PART I; 2024 Al Target)

Target Material	Particle Size (μ)	Carrier Gas Velocity (fps)	Range, Estimated Particle Velocity (fps)	Impactment Angle ($^\circ$)	Test Data: Target Weight Loss (mg/g)	Average Target Volume Loss ($\text{cm}^3 \times 10^{-3}$)	Weight Erosion Factor, e_w (mg/m)	Volume Erosion Factor, e_v ($\text{cm}^3 \times 10^{-3}/\text{gm}$)	Exponent (n) of Velocity Ratio: $(\frac{V_2}{V_1})^n$		Exponent (n) of Velocity Ratio: $(\frac{V_3}{V_2})^n$ or $(\frac{V_3}{V_1})^n$
									(E) Average Target Weight Loss Per Single Particle Impact ^a (mg/g $\times 10^{-6}$)	Ratio: $e_{21.5^\circ}^{21.5^\circ} / e_{60^\circ}^{60^\circ}$	
2024 Al (Annealed)	0-43	500	$V_1 = 480$	37.5	1.0	1.7	0.62	0.32	0.11	0.56	0.32 (1.6)
				60	1.1	1.1	0.40	0.20	0.074	0.56	0.20 --- ---
	0-43	685	$V_2 = 670$ 680/685	37.5	3.6	3.6	0.97	0.24	1.8	0.66	2.36 ---
				60	2.6	2.5	0.91	0.46	0.17	1.3	0.46 (1.5) 2.64 ---
	0-43	950	$V_3 = 925$ 900/950	37.5	4.4	4.2	1.5	0.70	2.1	0.76	1.42 0.48
				60	2.0	2.0	0.73	0.37	0.14	1.0	0.37 0.94 (-0.68)

^a Assuming the predominant erosive components are cubic particles of quartz (~70% wt or 3.78 gms, with edge dimensions equivalent to mean particle size).

Common Test Conditions

Arizona Road Dust; N = 5.40 gms
Dust Concentration: 40.0 mg/ft³
Carrier Gas: Compressed Air

Carrier Gas True Temperature: RT
Nozzle Dimensions: 1/4-inch I.D. x 10 ft. length

TABLE II B

Target Material	Particle Size (μ)	Carrier Gas Velocity (fpa)	Range, Estimated Particle Velocity (fpa)	Test Data; Target Weight Loss (mg/g)	Average Target Weight Loss ($\text{cm}^3 \times 10^{-3}$)	Weight Erosion Factor, ϵ_w (mg/g/gm)	Volume Erosion Factor, ϵ_v ($\text{cm}^3 \times 10^{-3}/\text{gm}$)	$\frac{\epsilon_v}{\epsilon_w}$	Average Target Weight Loss Per Single Particle Impact* ($\text{cm}^3 \times 10^{-11}$)	Exponent (α) of Velocity Ratio: $\left(\frac{v_2}{v_1}\right)^x$	Exponent (α) of Velocity Ratio: $\left(\frac{v_2}{v_1}\right)^x$	
								(a)	(b)	Ratio: $\frac{v_2}{v_1}$	Ratio: $\frac{v_2}{v_1}$	
2024 Al (Annealed)	43-74	525	$v_1 = 488$	475/500	37.5	2.1	0.77	0.39	0.14	29.	11.	(2.6)
						2.0	1.1	0.40	0.20	0.074	18.	5.5
						60	1.1	1.1	0.20			---
						37.5	3.9	3.8	1.4	0.70	52.	19.
						60	2.7	2.7	0.99	0.50	0.18	37.
						37.5	5.8	5.8	5.4	2.0	1.0	14.
						60	3.6	3.4	3.5	1.3	0.66	40.
						950	$v_3 = 880$	880/900				18.
						60						

* Assuming the predominant erosive components are cubic particles of quartz (~70% wt or 3.76 gm), with edge dimensions equivalent to mean particle size.

TABLE IIC

Target Material	Particle Size (μ)	Carrier Gas Velocity (ft/sec)	Range, Estimated Particle Velocity (ft/sec)	Impact Angle ($^\circ$)	Test Data: Target Weight Loss (mpa)	Average Target Volume Loss ($\text{cm}^3 \times 10^{-3}$)	Weight Erosion Factor, c (mpa/gm)	Volume Erosion Factor, c_v ($\text{cm}^3 \times 10^{-3}$ /gm)	Average Target Weight Loss Per Single Particle Impact (mpa $\times 10^{-3}$)	Exponent (n) of Velocity Ratio: $(\frac{v_2}{v_1})^n$	Exponent (n) of Velocity Ratio: $(\frac{v_3}{v_1})^n$ or $(\frac{v_2}{v_1})^n$
									Average Target Volume Loss Per Single Particle Impact (cm $^3 \times 10^{-3}$)	Ratio: $\frac{c_{37.5}}{c_{45.0}}$	Ratio: $\frac{c_{37.5}}{c_{45.0}}$
3036 Al (Annealed)	74-147	570	$v_1 = 488$	37.5	1.9	1.9	0.69	0.35	0.13	170.	61.
				60	0.9	0.9	0.33	0.17	0.011	65.	29.
				74-147	780	650/690	37.5	3.7	1.4	0.69	0.26
					60	2.4	2.5	0.91	0.46	0.17	220.
					74-147	950	$v_3 = 839$	37.5	4.8	1.7	0.85
						60	2.0	2.4	0.88	0.45	0.16
							2.6		210.	78.	1.85
											{-0.190}

* Assuming the predominant erosive components are cubic particles of quartz (~70% wt or 3.74 gmes), with edge dimensions equivalent to mean particle size.

TABLE II

Target Material	Particle Size (μ)	Carrier Gas Velocity (fps)	Median Particle Velocity (fps)	Range, Estimated Particle Velocity (fps)	Test Data: Target Weight Loss (mg/g)	Average Target Volume Loss ($\text{cm}^3 \times 10^{-3}$)	Weight Erosion Factor, f_w (mg/g/gm)	Volume Erosion Factor, f_v ($\text{cm}^3 \times 10^{-3}/\text{gm}$)	Average Target Weight Loss Per Single Particle Impact* (mg $\times 10^{-9}$)	Average Target Volume Loss Per Single Particle Impact* (cm $^3 \times 10^{-11}$)	Exponent (n) of Velocity Ratio: $\left(\frac{v_2}{v_1}\right)^x$	Exponent (n) of Velocity Ratio: $\left(\frac{v_3}{v_1}\right)^x$ or $\left(\frac{v_3}{v_2}\right)^x$
											Ratio: $\frac{f_w}{f_v}$	Ratio: $\frac{f_w}{f_v}$
2024 Al (Annealed)	147-208	605	$v_1 = 480$	475/500	37.5	1.9	0.69	0.35	0.13	670.	240.	(1.6)
					60	1.9	1.0	0.37	0.19	360.	130.	---
					60	1.0	0.9	0.26	0.098	1400.	490.	(2.6)
					60	3.9	3.9	1.4	0.72	1400.	490.	2.23
					60	3.8	1.3	0.51	0.26	1600.	560.	1.14
					60	1.4	1.4	0.51	0.094	1600.	560.	---
					60	1.4	1.4	0.51	0.30	1600.	560.	1.92
					60	4.6	4.4	1.6	0.62	1600.	560.	1.06
					60	4.2	2.6	2.4	0.44	1600.	560.	4.79
					60	4.2	2.6	2.2	0.16	310.	2.00	4.79

- Assuming the predominant erosive components are cubic particles of quartz (~70% wt or 3.78 gms), with edge dimensions equivalent to mean particle size.

TABLE IIIA

COMPILED TEST DATA (PART I; Ti-6Al-4V Target)

Assuming the predominant erosive components are cubic particles of quartz (~70% wt or 3.78 gms), with edge dimensions equivalent to mean particle size.

TABLE III B

Target Material	Particle Size (μ)	Carrier Gas Velocity (fps)	Median Particle Velocity (fps)	Range, Estimated Particle Velocity (fps)	Test Data: Target Weight Loss (mg/s)	Average Target Volume Loss ($\text{cm}^3 \times 10^{-3}$)	Weight Erosion Factor, ϵ_w (mg/s/grm)	Volume Erosion Factor, ϵ_v ($\text{cm}^3 \times 10^{-3}/\text{gm}$)	Average Target Weight Loss Per Single Particle Impact* (mgs $\times 10^{-8}$)		Ratio: $\frac{\epsilon_v}{\epsilon_w}$ or $\left(\frac{v_3}{v_1}\right)^x$	Exponent (x) of Velocity Ratio: $\left(\frac{v_2}{v_1}\right)^x$ or $\left(\frac{v_3}{v_1}\right)^x$
									Average Target Volume	Loss Per Single Particle Impact*		
Ti-4Al-4V (Annealed)	43-74	525	$v_1 = 488$	475/500	37.5	2.3	0.52	0.43	0.096	32.	7.1	(1.5)
					60	1.4	1.5	0.34	0.28	0.063	21.	4.7
						1.5					(1.1)	—
	43-74	725	$v_2 = 670$	650/690	37.5	3.9	0.88	0.72	0.16	53.	12.	1.69
					60	3.6	3.4	0.77	0.63	0.14	47.	11.
						3.2					(1.1)	2.60
	43-74	950	$v_3 = 880$	860/900	37.5	7.2	6.9	1.6	1.3	0.30	95.	22.
					60	5.0	5.3	1.2	0.98	0.22	73.	16.
						5.6						1.65

* Assuming the predominant erosive components are cubic particles of quartz (~70% wt or 3.76 gms), with edge dimensions equivalent to mean particle size.

TABLE III C

Target Material	Particle Size (μ)	Carrier Gas Velocity (ft/sec)	Range, Estimated Particle Velocity (ips)	Impingement Angle ($^\circ$)	Test Data: Target Weight Loss (mgs)	Average Target Weight Loss ($\times 10^{-3}$)	Weight Erosion Factor, e_w (mgs/gm)	Volume Erosion Factor, e_v ($\text{cm}^3 \times 10^{-3}/\text{gm}$)	Average Target Volume Loss Per Single Particle Impact* (mgs $\times 10^{-9}$)	Exponent (n) of Velocity Ratio: $(\frac{v_2}{v_1})^n$		Ratio: $(\frac{v_1}{v_2})^n$ or $(\frac{e_w}{e_v})^n$	
										Average Target Volume Loss Per Single Particle Impact* (mgs $\times 10^{-9}$)	Average Target Volume Loss Per Single Particle Impact* (mgs $\times 10^{-9}$)		
74-147 (Alumina)	570	$V_1 = 480$	475/500	37.5	2.5	2.4	0.54	0.44	0.10	210.	48.	(1.2)	
	760	$V_2 = 670$	650/690	60	1.8	1.9	0.43	0.35	0.060	170.	36.	—	
	74-147	760	$V_3 = 630$	755/865	37.5	4.3	4.3	0.97	0.80	0.18	380.	86.	(1.2)
	550			60	3.5	3.6	0.81	0.67	0.15	350.	72.	2.04	
	74-147			37.5	5.6	5.8	1.3	1.1	0.24	510.	120.	1.66	
	60				6.0	5.6	1.2	1.0	0.22	440.	110.	1.98	
					5.4								

* Assuming the predominant erosive components are cubic particles of quartz (~70% wt or 3.76 grams), with edge dimensions equivalent to mean particle size.

TABLE III D

Target Material	Particle Size (μ)	Carrier Gas Velocity (fps)	Median Particle Velocity (fps)	Range, Estimated Particle Velocity (fps)	Impingement Angle ($^\circ$)	Test Data: Target Weight Loss (mg/g)	Average Target Volume Loss ($\text{cm}^3 \times 10^{-3}$)	Weight Erosion Factor, ϵ_w (mg/g)	Volume Erosion Factor, ϵ_v ($\text{cm}^3 \times 10^{-3}/\text{gm}$)	Average Target Weight Loss Per Single Particle Impact* (mgas $\times 10^{-5}$)		Ratio: $\frac{\epsilon_v}{\epsilon_w}$	Exponent (n) of Velocity Ratio: $\left(\frac{V_2}{V_1}\right)^n$	Exponent (n) of Velocity Ratio: $\left(\frac{V_3}{V_1}\right)^n$	Ratio: $\frac{\epsilon_v}{\epsilon_w}$	Exponent (n) of Velocity Ratio: $\left(\frac{V_2}{V_2}\right)^n$
										Average Target Weight Loss Per Single Particle Impact* (mgas $\times 10^{-5}$)	Average Target Weight Loss Per Single Particle Impact* (mgas $\times 10^{-5}$)					
Tl-6Al-4V (Annealed)	147-206	605	$V_1 = 486$	475/500	37.5	2.4	0.54	0.44	0.10	850.	180.	(1.2)	—	—	—	
					60	2.0	0.45	0.37	0.043	700.	160.	(1.2)	—	—	—	
	147-206	835	$V_2 = 670$	650/695	37.5	4.0	4.1	0.93	0.76	0.17	1400.	350.	(1.4)	1.67	—	—
					60	2.8	2.9	0.66	0.54	0.12	1000.	250.	(1.4)	1.16	—	—
	147-206	950	$V_3 = 754$	715/795	37.5	5.8	5.9	1.3	1.1	0.24	2100.	460.	(1.2)	2.05	3.23	—
					60	4.8	5.1	1.2	0.94	0.22	1800.	450.	(1.2)	2.14	5.48	—

* Assuming the predominant erosive components are cubic particles of quartz (~70% wt or 2.76 gms), with edge dimensions equivalent to mean particle size.

TABLE IV

COMPILED LIST OF SENTS IN TEST DATA (PART I: 410 SS Targets)

TABLE IVB

Target Material	Particle Size (μ)	Carrier Gas Velocity (fps)	Medium Particle Velocity (fps)	Range Estimated	Impact Angle (°)	Test Data:	Average Target Weight Loss (mg/s)	Average Target Volume Loss (cm³/s × 10⁻²)	Weight Erosion Factor, ϵ_w (mg/s/cm)	Volume Erosion Factor, ϵ_v (cm³/s × 10⁻³/gm)	Average Target Weight Loss Per Single Particle Impact, ϵ_{sp} (mg/s × 10⁻⁹)	Exponent (n) of Velocity Ratio, $(\frac{v_2}{v_1})^n$	Exponent (n) of Velocity Ratio, $(\frac{v_3}{v_1})^n$ or $(\frac{v_2}{v_1})^n$	
							(mg/s)	(cm³/s × 10⁻²)	(mg/s/cm)	(cm³/s × 10⁻³/gm)	(mg/s × 10⁻⁹)	(v ₂ /v ₁) ⁿ	(v ₃ /v ₁) ⁿ or (v ₂ /v ₁) ⁿ	
410 MM (diamond)	45-74	525	V ₁ = 468	475/500	37.5	2.2	2.2	0.20	0.41	0.052	30.	3.0	—	
						60	1.5	1.5	0.19	0.28	0.035	21.	2.6	(1.5)
						60	1.5	1.5	0.54	0.78	0.10	58.	7.4	—
						60	3.6	3.6	0.46	0.67	0.005	49.	6.3	—
						60	3.6	3.6	0.78	1.1	0.14	84.	11.	—
						60	5.4	5.4	0.66	0.98	0.13	73.	9.3	—
						60	5.4	5.4	—	—	—	2.15	2.15	—
						60	—	—	—	—	—	—	—	—

Assuming the predominant erosive component are cubic particles of quartz (~70% or 2.75 g/cm³, with edge dimensions equivalent to mean particle size).

TABLE IVC

Target Material	Particle Size #4	Carrier Gas Velocity (ft/sec)	Range- Estimated Particle Velocity (ft/sec)	Test Data: Target Weight Loss (mg)	Average Target Volume Loss (cm ³ x 10 ⁻³)	Weight Erosion Factor-a (mg/gm)	Volume Erosion Factor, C, (cm ³ x 10 ⁻³ /gm)	Average Target Weight Loss Per Single Particle Impact*	Average Target Volume Loss Per Single Particle Impact Ratio: c _{37.5} / c ₆₀ *	Exponent (n) Ratio: $\left(\frac{v_2}{v_1}\right)^n$	Exponent (n) Ratio: $\left(\frac{v_2}{v_1}\right)^n$ or $\left(\frac{v_2}{v_1}\right)^n$ Ratio: $\left(\frac{v_2}{v_1}\right)^n$
								Impact* (mpa x 10 ⁻⁶)	(cm ³ x 10 ⁻¹¹)	(1.7)	(1.7)
Aluminum (Anodized)	74-167	870	V ₁ = 400	473/500	37.5	2.3	0.31	0.44	0.037	210.	27.
					60	2.4	0.31	0.44	0.044	170.	21.
					60	1.9	0.24	0.36	0.044	—	—
					60	1.8	0.24	0.36	0.044	—	—
					60	4.4	0.54	0.83	0.11	450.	51.
					60	3.7	0.47	0.80	0.087	350.	42.
					60	3.7	0.47	0.80	0.087	42.	2.12
					700	V ₂ = 670	653/600	37.5	—	—	—
					60	4.5	0.54	0.83	0.11	—	—
					60	3.7	0.47	0.80	0.087	—	—
					60	3.7	0.47	0.80	0.087	—	—
					700	V ₃ = 630	703/600	37.5	—	—	—
					60	6.4	0.62	1.2	0.15	570.	73.
					60	6.4	0.62	1.2	0.15	570.	73.
					60	5.2	0.58	0.96	0.13	470.	60.
					60	5.4	0.60	1.00	0.13	470.	60.

a Assuming the predominant erosive components are cubic particles of quartz
 b 700 or 3.76 gram, with edge dimensions equivalent to mean particle size.

TABLE IV D

Target material	Particle size (μ)	Carrier Gas Velocity (ft/sec)	Range Estimated Particle Velocity (ft/sec)	Test Data: Impact Angle (°)	Average Target Weight Loss (mg/sec)	Average Target Volume Loss ($\text{cm}^3 \times 10^{-3}$)	Weight Erosion Factor, α (mg/sec/gm)	Volume Erosion Factor, β ($\text{cm}^3 \times 10^{-3}/\text{gm}$)	Average Target Weight Loss Per Single Particle Impact* (mg/sec $\times 10^{-3}$)	Average Target Volume Loss Per Single Particle Impact* (cm $^3 \times 10^{-11}$)	Exponent (n) of Velocity Ratio: $(\frac{V_2}{V_1})^n$ or $(\frac{V_1}{V_2})^n$	Exponent (n) of Velocity Ratio: $(\frac{V_2}{V_1})^n$ or $(\frac{V_1}{V_2})^n$	
									Ratio: $0.375/0.67$	Ratio: $0.375/0.67$	Ratio: $0.375/0.67$	Ratio: $0.375/0.67$	
Alumina (Al ₂ O ₃)	147-300	665	V ₁ = 460	475/500	37.5	2.4	0.31	0.44	0.057	110.	(1.1)	—	
					60	2.0	0.27	0.39	0.060	740.	95.	—	
					147-300	635	37.5	4.1	0.54	0.78	0.10	150.	
						60	3.0	0.38	0.56	0.070	1100.	130.	
						147-300	660	715/750	37.5	5.9	0.76	1.1	0.14
							60	4.0	0.63	0.91	0.12	1700.	210.
							5.0						

* Assuming the predominant erosive components are cubic particles of quartz (~75 μ or 3.75 gm), with edge dimensions equivalent to mean particle size.

TABLE VA

COMPILATION OF SERIES III TEST DATA (PART I; 17-7 PH Target)

Target Material	P _g (psi) Rate (in.)	Carrier Gas Velocity (ft/sec)	Range Estimated Particle Velocity (ft/sec)	Implantation Angle (°)	Test Data: Target Weight Loss (mg/m)	Average Target Weight Loss (mg/m)	Average Target Volume Loss (cm ³) x 10 ⁻³	Weight Erosion Factor, $\frac{V_2}{V_1}$ (mg/m ²)	Average Target Weight Loss Per Single Particle Impact*		Average Target Volume Loss Per Single Particle Impact*	
									Average Target Weight Loss Per Single Particle Impact* (mgs x 10 ⁻⁶)	Ratio ("27.5") or $\left(\frac{V_2}{V_1}\right)^n$	Average Target Volume Loss Per Single Particle Impact* (cm ³ x 10 ⁻¹³)	Ratio ("27.5") or $\left(\frac{V_2}{V_1}\right)^n$
17-7 PH (annealed)	0-43	500	V ₁ = 480	37.5	2.0	2.1	0.39	0.39	0.663	1.1	0.14	0.19
					60	1.4	1.3	0.17	0.34	0.633	0.44	0.077
					60	1.2	1.0	0.22	0.72	0.604	2.0	0.26
					60	2.0	2.0	0.39	0.54	0.672	1.5	0.30
					60	2.0	2.0	0.73	1.0	0.37	0.39	0.39
					60	4.4	4.3	0.57	0.89	0.11	2.2	1.06
					60	4.4	4.3	0.57	0.89	0.29	1.19	1.19
					60	4.4	4.3	0.57	0.89	0.39	1.06	1.06

* Assuming the predominant erosive components are cubic particles of quartz (~795 wt or 3.78 gram), with edge dimensions equivalent to mean particle size.

TABLE VB

Target Material	Particle Size (μ)	Carrier Gas Velocity (ft/sec)	Median Particle Velocity (ft/sec)	Range, Estimated Particle Velocity (ft/sec)	Impingement Angle (°)	Test Data: Target Weight Loss (mg/s)	Average Target Volume Loss (cm ³ × 10 ⁻³)	Weight Erosion Factor, ϵ (mg/s/cm)	Volume Erosion Factor, ϵ_v (cm ³ × 10 ⁻³ /gm)	Average Target Weight Loss Per Single Particle Impact* (mg/s × 10 ⁻⁹)	Average Target Volume Loss Per Single Particle Impact* (cm ³ × 10 ⁻⁹)	Exponent (n) of Velocity Ratio: $\left(\frac{v_2}{v_1}\right)^n$	Exponent (n) of Velocity Ratio: $\left(\frac{v_2}{v_1}\right)^n$ or $\left(\frac{v_1}{v_2}\right)^n$	Exponent (n) of Velocity Ratio: $\left(\frac{v_2}{v_1}\right)^n$ or $\left(\frac{v_1}{v_2}\right)^n$
										33.	4.4	(1.6)	—	—
17.4 μm (Assumed)	45-74	500	v ₁ = 400	475/500	37.5	2.3	2.4	0.32	0.44	0.059	33.	4.4	—	—
					60	1.4	1.5	0.20	0.28	0.037	21.	2.7	—	—
					1.5	1.5	—	—	—	—	—	—	—	—
					60	3.6	3.7	0.49	0.66	0.001	51.	6.7	—	—
					37.5	4.2	4.3	0.57	0.80	0.11	59.	7.8	1.85	—
					60	5.6	5.7	0.49	0.66	0.001	51.	6.7	(1.2)	2.05
					37.5	4.3	4.3	0.57	0.80	0.11	59.	7.8	—	—
					60	5.6	5.7	0.49	0.66	0.001	51.	6.7	—	—
					37.5	4.2	4.3	0.57	0.80	0.11	59.	7.8	—	—
					60	5.6	5.7	0.49	0.66	0.001	51.	6.7	—	—
					37.5	4.3	4.3	0.57	0.80	0.11	59.	7.8	—	—
					60	5.6	5.7	0.49	0.66	0.001	51.	6.7	—	—
					37.5	4.2	4.3	0.57	0.80	0.11	59.	7.8	—	—
					60	5.6	5.7	0.49	0.66	0.001	51.	6.7	—	—
					37.5	4.3	4.3	0.57	0.80	0.11	59.	7.8	—	—
					60	5.6	5.7	0.49	0.66	0.001	51.	6.7	—	—
					37.5	4.2	4.3	0.57	0.80	0.11	59.	7.8	—	—
					60	5.6	5.7	0.49	0.66	0.001	51.	6.7	—	—
					37.5	4.3	4.3	0.57	0.80	0.11	59.	7.8	—	—
					60	5.6	5.7	0.49	0.66	0.001	51.	6.7	—	—
					37.5	4.2	4.3	0.57	0.80	0.11	59.	7.8	—	—
					60	5.6	5.7	0.49	0.66	0.001	51.	6.7	—	—
					37.5	4.3	4.3	0.57	0.80	0.11	59.	7.8	—	—
					60	5.6	5.7	0.49	0.66	0.001	51.	6.7	—	—
					37.5	4.2	4.3	0.57	0.80	0.11	59.	7.8	—	—
					60	5.6	5.7	0.49	0.66	0.001	51.	6.7	—	—
					37.5	4.3	4.3	0.57	0.80	0.11	59.	7.8	—	—
					60	5.6	5.7	0.49	0.66	0.001	51.	6.7	—	—
					37.5	4.2	4.3	0.57	0.80	0.11	59.	7.8	—	—
					60	5.6	5.7	0.49	0.66	0.001	51.	6.7	—	—
					37.5	4.3	4.3	0.57	0.80	0.11	59.	7.8	—	—
					60	5.6	5.7	0.49	0.66	0.001	51.	6.7	—	—
					37.5	4.2	4.3	0.57	0.80	0.11	59.	7.8	—	—
					60	5.6	5.7	0.49	0.66	0.001	51.	6.7	—	—
					37.5	4.3	4.3	0.57	0.80	0.11	59.	7.8	—	—
					60	5.6	5.7	0.49	0.66	0.001	51.	6.7	—	—
					37.5	4.2	4.3	0.57	0.80	0.11	59.	7.8	—	—
					60	5.6	5.7	0.49	0.66	0.001	51.	6.7	—	—
					37.5	4.3	4.3	0.57	0.80	0.11	59.	7.8	—	—
					60	5.6	5.7	0.49	0.66	0.001	51.	6.7	—	—
					37.5	4.2	4.3	0.57	0.80	0.11	59.	7.8	—	—
					60	5.6	5.7	0.49	0.66	0.001	51.	6.7	—	—
					37.5	4.3	4.3	0.57	0.80	0.11	59.	7.8	—	—
					60	5.6	5.7	0.49	0.66	0.001	51.	6.7	—	—
					37.5	4.2	4.3	0.57	0.80	0.11	59.	7.8	—	—
					60	5.6	5.7	0.49	0.66	0.001	51.	6.7	—	—
					37.5	4.3	4.3	0.57	0.80	0.11	59.	7.8	—	—
					60	5.6	5.7	0.49	0.66	0.001	51.	6.7	—	—
					37.5	4.2	4.3	0.57	0.80	0.11	59.	7.8	—	—
					60	5.6	5.7	0.49	0.66	0.001	51.	6.7	—	—
					37.5	4.3	4.3	0.57	0.80	0.11	59.	7.8	—	—
					60	5.6	5.7	0.49	0.66	0.001	51.	6.7	—	—
					37.5	4.2	4.3	0.57	0.80	0.11	59.	7.8	—	—
					60	5.6	5.7	0.49	0.66	0.001	51.	6.7	—	—
					37.5	4.3	4.3	0.57	0.80	0.11	59.	7.8	—	—
					60	5.6	5.7	0.49	0.66	0.001	51.	6.7	—	—
					37.5	4.2	4.3	0.57	0.80	0.11	59.	7.8	—	—
					60	5.6	5.7	0.49	0.66	0.001	51.	6.7	—	—
					37.5	4.3	4.3	0.57	0.80	0.11	59.	7.8	—	—
					60	5.6	5.7	0.49	0.66	0.001	51.	6.7	—	—
					37.5	4.2	4.3	0.57	0.80	0.11	59.	7.8	—	—
					60	5.6	5.7	0.49	0.66	0.001	51.	6.7	—	—
					37.5	4.3	4.3	0.57	0.80	0.11	59.	7.8	—	—
					60	5.6	5.7	0.49	0.66	0.001	51.	6.7	—	—
					37.5	4.2	4.3	0.57	0.80	0.11	59.	7.8	—	—
					60	5.6	5.7	0.49	0.66	0.001	51.	6.7	—	—
					37.5	4.3	4.3	0.57	0.80	0.11	59.	7.8	—	—
					60	5.6	5.7	0.49	0.66	0.001	51.	6.7	—	—
					37.5	4.2	4.3	0.57	0.80	0.11	59.	7.8	—	—
					60	5.6	5.7	0.49	0.66	0.001	51.	6.7	—	—
					37.5	4.3	4.3	0.57	0.80	0.11	59.	7.8	—	—
					60	5.6	5.7	0.49	0.66	0.001	51.	6.7	—	—
					37.5	4.2	4.3	0.57	0.80	0.11	59.	7.8	—	—
					60	5.6	5.7	0.49	0.66	0.001	51.	6.7	—	—
					37.5	4.3	4.3	0.57	0.80	0.11	59.	7.8	—	—
					60	5.6	5.7	0.49	0.66	0.001	51.	6.7	—	—
					37.5	4.2	4.3	0.57	0.80	0.11	59.	7.8	—	—
					60	5.6	5.7	0.49	0.66	0.001	51.	6.7	—	—
					37.5	4.3	4.3	0.57	0.80	0.11	59.	7.8	—	—
					60	5.6	5.7	0.49	0.66	0.001	51.	6.7	—	—
					37.5	4.2	4.3	0.57	0.80	0.11	59.	7.8	—	—
					60	5.6	5.7	0.49	0.66	0.001	51.	6.7	—	—
					37.5	4.3	4.3	0.57	0.80	0.11	59.	7.8	—	—
					60	5.6	5.7	0.49	0.66	0.001	51.	6.7	—	—
					37.5	4.2	4.3	0.57	0.80	0.11	59.	7.8	—	—
					60	5.6	5.7	0.49	0.66	0.001	51.	6.7	—	—
					37.5	4.3	4.3	0.57	0.80	0.11	59.	7.8	—	—
					60	5.6	5.7	0.49	0.66	0.001	51.	6.7	—	—
					37.5	4.2	4.3	0.57	0.80	0.11	59.	7.8	—	—
					60	5.6	5.7	0.49	0.66	0.001	51.	6.7	—	—
	</td													

TABLE VC

Target Material	Particle Size (μ)	Carrier Gas Velocity (ft/sec)	Range- Estimated Particle Velocity (ft/sec)	Impact Angle (°)	Test Data: Target Weight Loss (mg/sec)	Average Target Volume Loss (cm ³ × 10 ⁻³)	Weight Erosion Factor, f_w (mg/sec/gm)	Volume Erosion Factor, f_v (cm ³ × 10 ⁻³ /sec)	Exponent (n) of Velocity Ratio: $\left(\frac{v_2}{v_1}\right)^n$		Exponent (n) of Velocity Ratio: $\left(\frac{v_2}{v_1}\right)^n$ or $\left(\frac{v_2}{v_1}\right)^n$
									Average Target Weight Loss Per Single Particle Impact (mg/sec)	Average Target Volume Loss Per Single Particle Impact (cm ³ × 10 ⁻³)	
17-7 PH (Aluminum)	74-147	570	$v_1 = 460$	478/600	37.5	2.3	2.4	0.32	0.44	0.600	210.
					60	1.9	1.9	0.25	0.35	0.600	170.
					74	1.9	1.9	0.41	0.65	0.11	410.
					74-147	700	$v_2 = 670$	650/600	37.5	4.6	34.
					60	3.9	3.9	0.32	0.72	0.000	2.17
					60	3.9	3.9	0.32	0.72	360.	2.38
					74-147	900	$v_3 = 820$	700/600	37.5	6.3	0.16
					60	5.0	5.0	0.77	1.1	50.	1.07
									0.14	0.11	2.10
									0.0	0.0	1.00

* Assuming the predominant erosive component are cubic particles of quartz (~70% or 2.70 gm/cm³), with edge dimensions equivalent to mean particle size.

TABLE VD

Target Material	Particle Size (μ)	Carrier Gas Velocity (ft/sec)	Medium Particle Velocity (ft/sec)	Range, Estimated Particle Velocity (ft/sec)	Test Data: Target Weight Loss (mg/m)	Average Target Weight Loss (mg/m)	Weight Erosion Factor ^a (mg/cm ²)	Volume Erosion Factor ^b (cm ³ × 10 ⁻³ /cm)	Exponent of Velocity Ratio, $(\frac{v_1}{v_2})^n$		Exponent of Velocity Ratio, $(\frac{v_2}{v_3})^n$	
									Average Target Weight Loss Per Single Particle Impact (cm ² × 10 ⁻¹¹)	Ratio, $\frac{v_1}{v_2}$	Average Target Weight Loss Per Single Particle Impact (mg × 10 ⁻⁶)	Ratio, $\frac{v_2}{v_3}$
Si-T-Si (sandblasted)	167-300	605	$v_1 = 460$	475/500	37.5	2.4	0.33	0.46	0.001	0.21	—	—
		635	$v_2 = 670$	650/665	60	2.2	0.21	0.28	0.39	0.002	0.20	—
		167-300	635	685/700	37.5	4.2	0.32	0.56	0.78	0.10	200.	1.01
		605	$v_3 = 715$	715/735	60	3.2	0.23	0.44	0.61	0.003	100.	0.21
		605	$v_1 = 460$	475/500	37.5	6.0	0.1	0.81	1.1	0.15	200.	2.04
		635	$v_2 = 670$	650/665	60	5.2	0.1	0.68	0.94	0.13	100.	0.09

^a Assuming the primary erosive components are cubic particles of quartz (~0.96 or 3.78 gm/cm³), with edge dimensions equivalent to mean particle size.

$n_{1,2}; n_{1,3}; n_{1,4}$
 Derived from the
 typical equation

Particle Size (μ)	Measured Slope (m)	$C_{(1,2,3,4)} = K\rho \Delta^n_{(1,2,3,4)}$	$\left[\frac{C_2}{C_1} = \left(\frac{\Delta_2}{\Delta_1} \right)^{n_{1,2}} \right]$
0-43 (subscript 1)	1.66	$C_1 = 8.47 \times 10^{-17}$	-----
43-74 (subscript 2)	1.75	$C_2 = 1.46 \times 10^{-15}$	$n_{1,2} = 0.897$
74-147 (subscript 3)	1.68	$C_3 = 1.55 \times 10^{-14}$	$n_{1,3} = 1.02$
147-208 (subscript 4)	1.89	$C_4 = 1.60 \times 10^{-14}$	$n_{1,4} = 0.804$
Average Value	1.75	-----	0.907

Based upon this preliminary analysis, the equation for the relationship of E_V and particle energy might be written,

$$E_V = K\rho (\Delta V^2)^{0.9} \quad (3)$$

The reasonably good reproducibility of the exponent, m , in the analysis above, contrasts markedly with the wide and apparently random scatter of the velocity exponents (x) listed in Tables II, III, IV, & V. Here, the ratio of erosion factors represented by individual data points (constant particle size and incidence angle) is equated to the corresponding ratio of particle velocities raised to a power, x . The exponent, x , ranges more or less randomly between (-) 0.68 and +5.48. The problem in not defining a more reproducible exponent by this method may arise from taking too restricted a view of available data. Each ratio selected comes from within a rather narrow range of particle energies, relative to the total range of particle energies tested. Moreover, each data point is the average of duplicate testing only, whereas data from 24 tests is available for each target material and impingement angle combination. To obtain better data averaging, log-log plots of E_V versus ΔV^2 ($\propto MV^2$) were drawn using all available data for each target-angle combination, see Figures 11 through 18. The correlations between E_V and ΔV^2 for all combinations of test variables proved remarkably good and very similar, as demonstrated by the linearity of the curves and by the calculated values for $K\rho$ and the exponent, y (equation (4)), derived from analysis of the curves, using the relation

2024-Al (ANNEALED)
37.5°
A. R. DUST

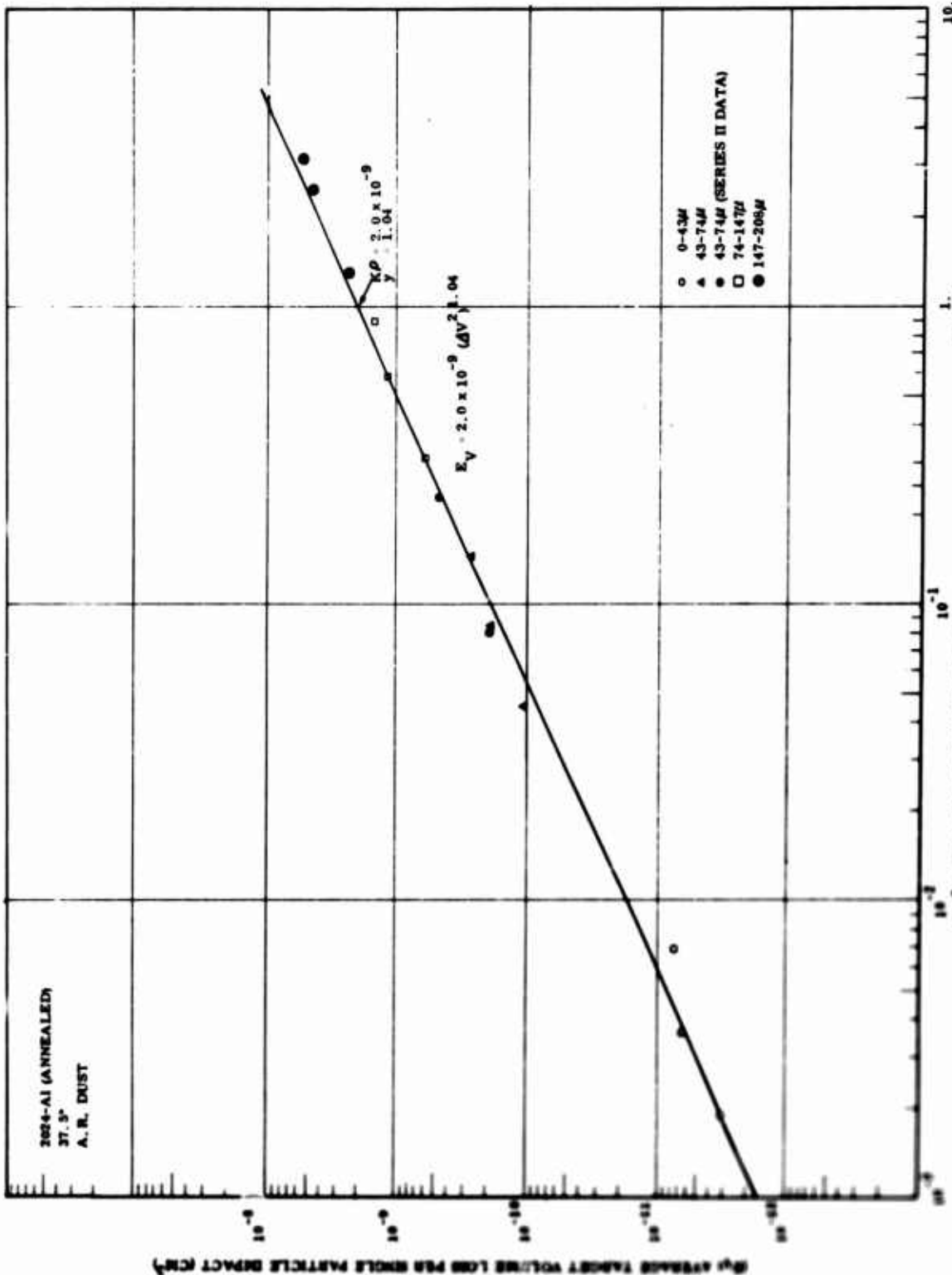


FIGURE 11. AVERAGE TARGET VOLUME LOSS PER SINGLE PARTICLE IMPACT (\bar{E}_V) VERSUS δv^2

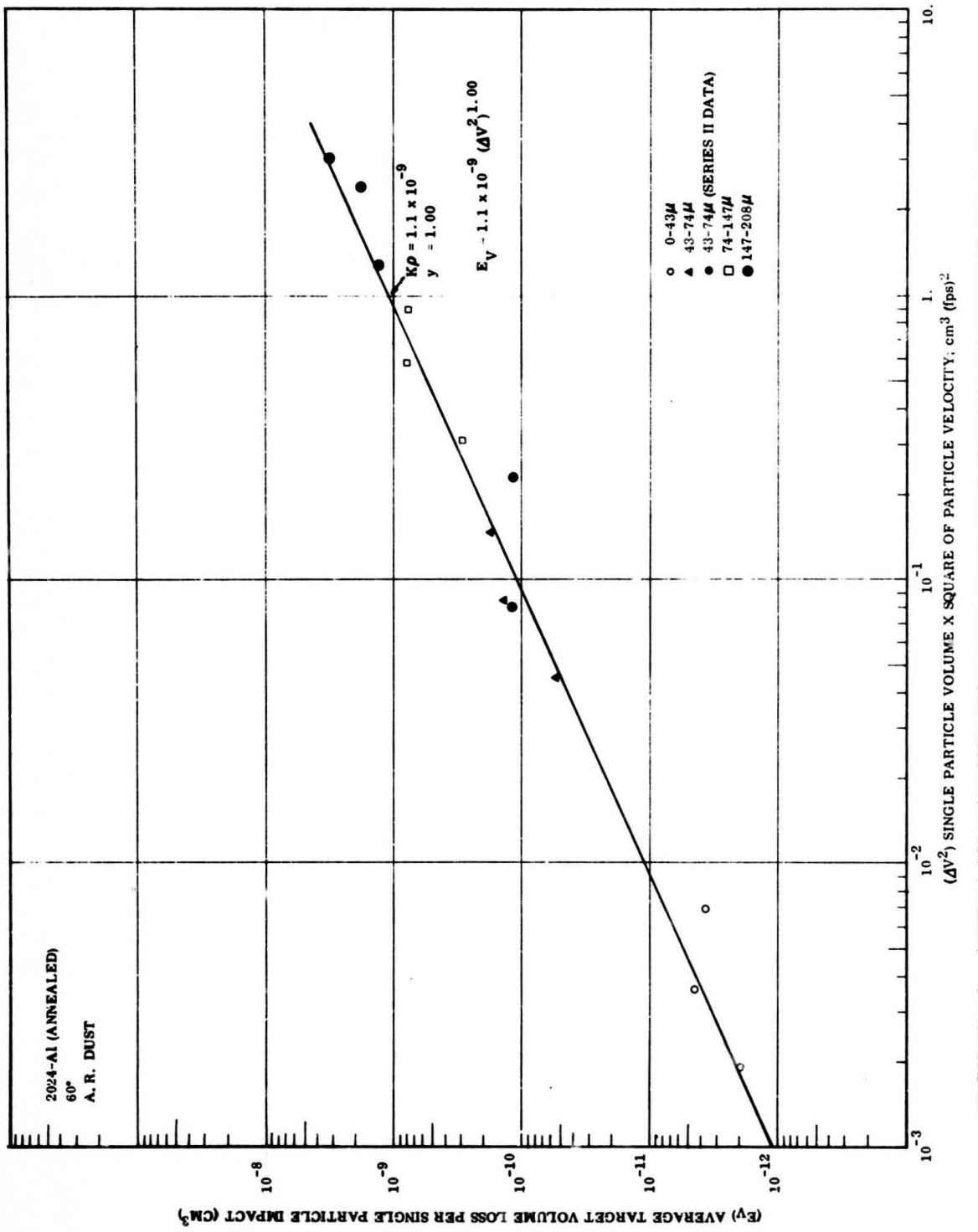
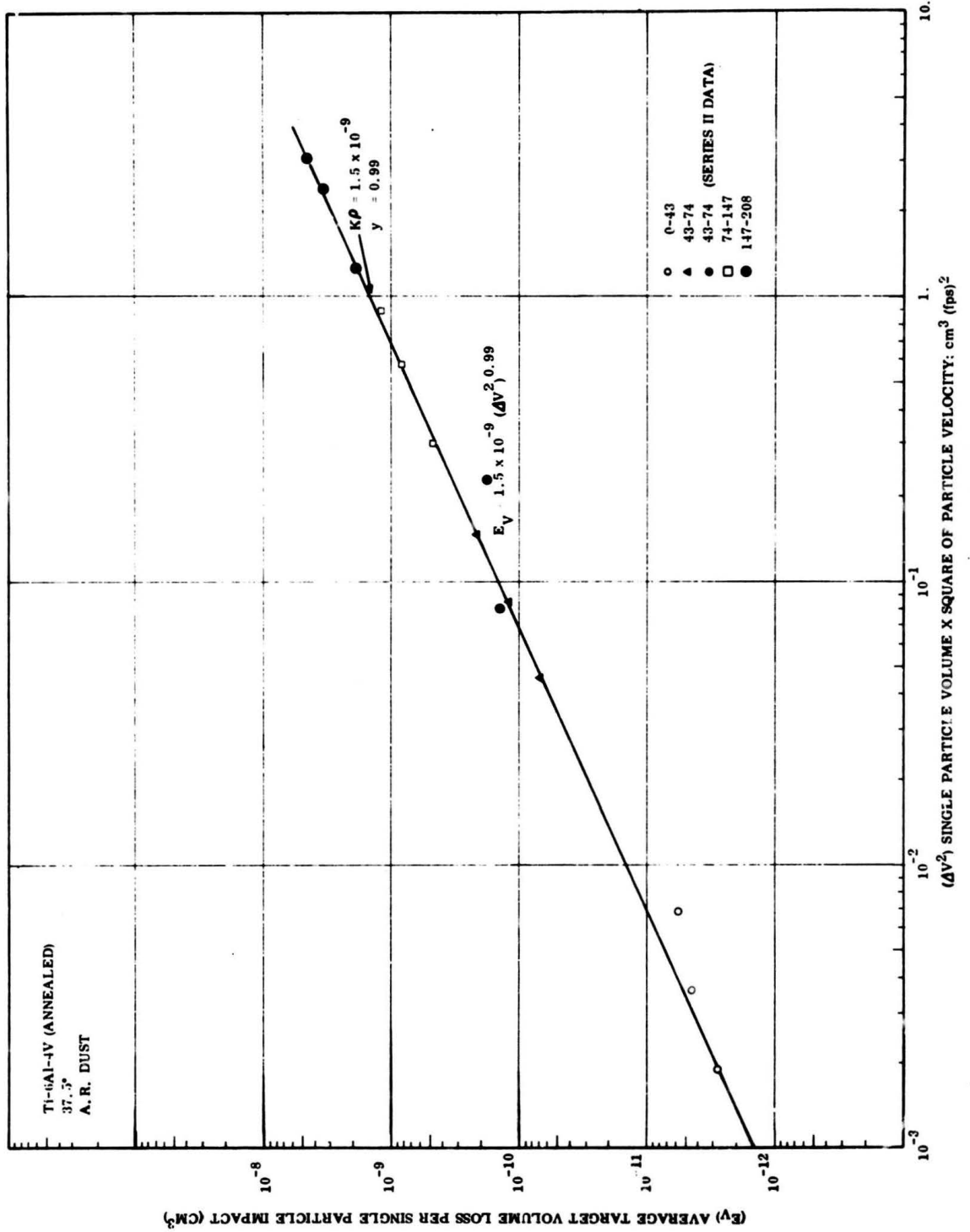


FIGURE 12. AVERAGE TARGET VOLUME LOSS PER SINGLE PARTICLE IMPACT (E_V) VERSUS ΔV^2



**FIGURE 13. AVERAGE TARGET VOLUME LOSS PER SINGLE PARTICLE IMPACT
 (E_V) VERSUS ΔV^2**

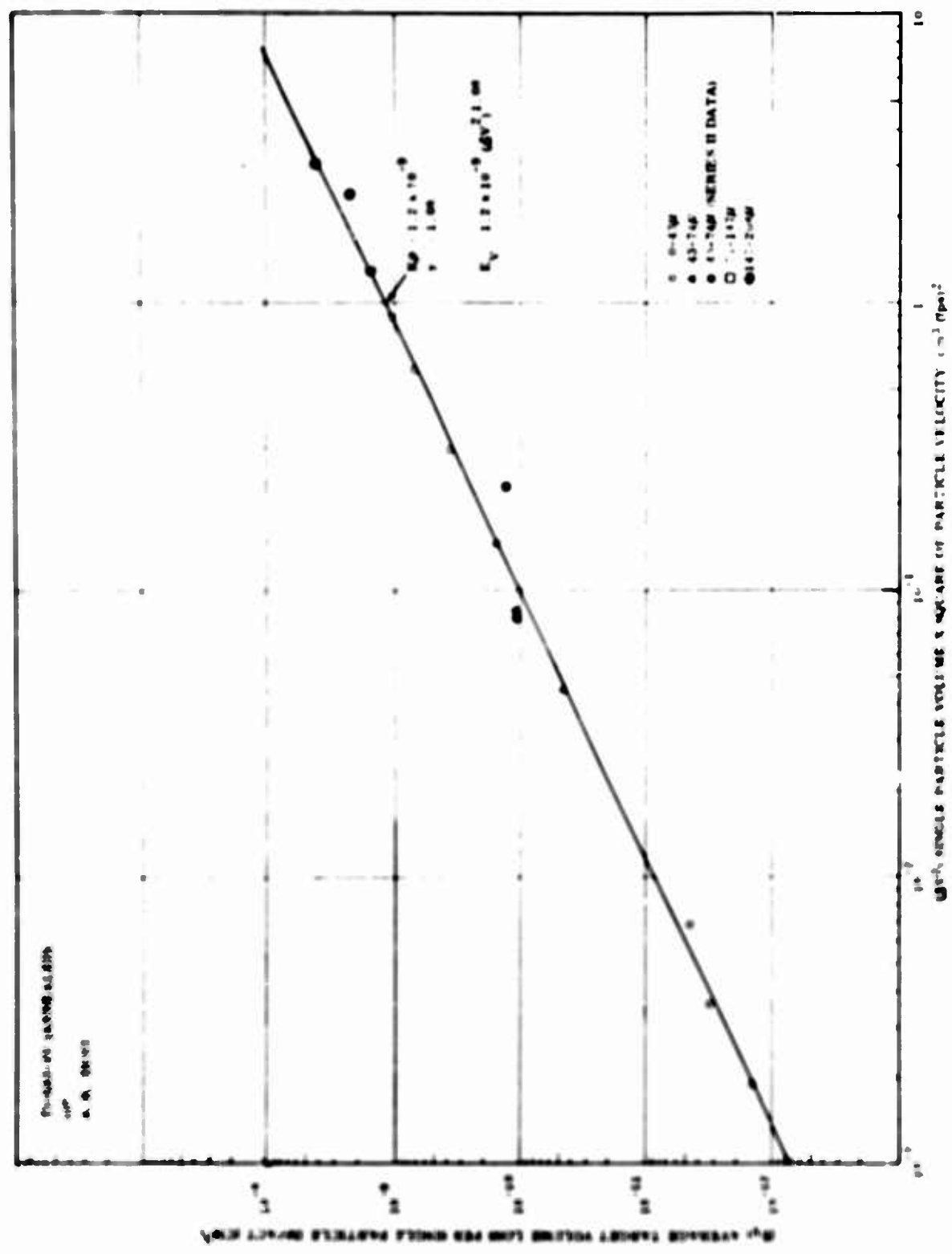


FIGURE 14. AVERAGE TARGET VOLUME LOSS PER SINGLE PARTICLE IMPACT (F_V) VERSUS Av^2

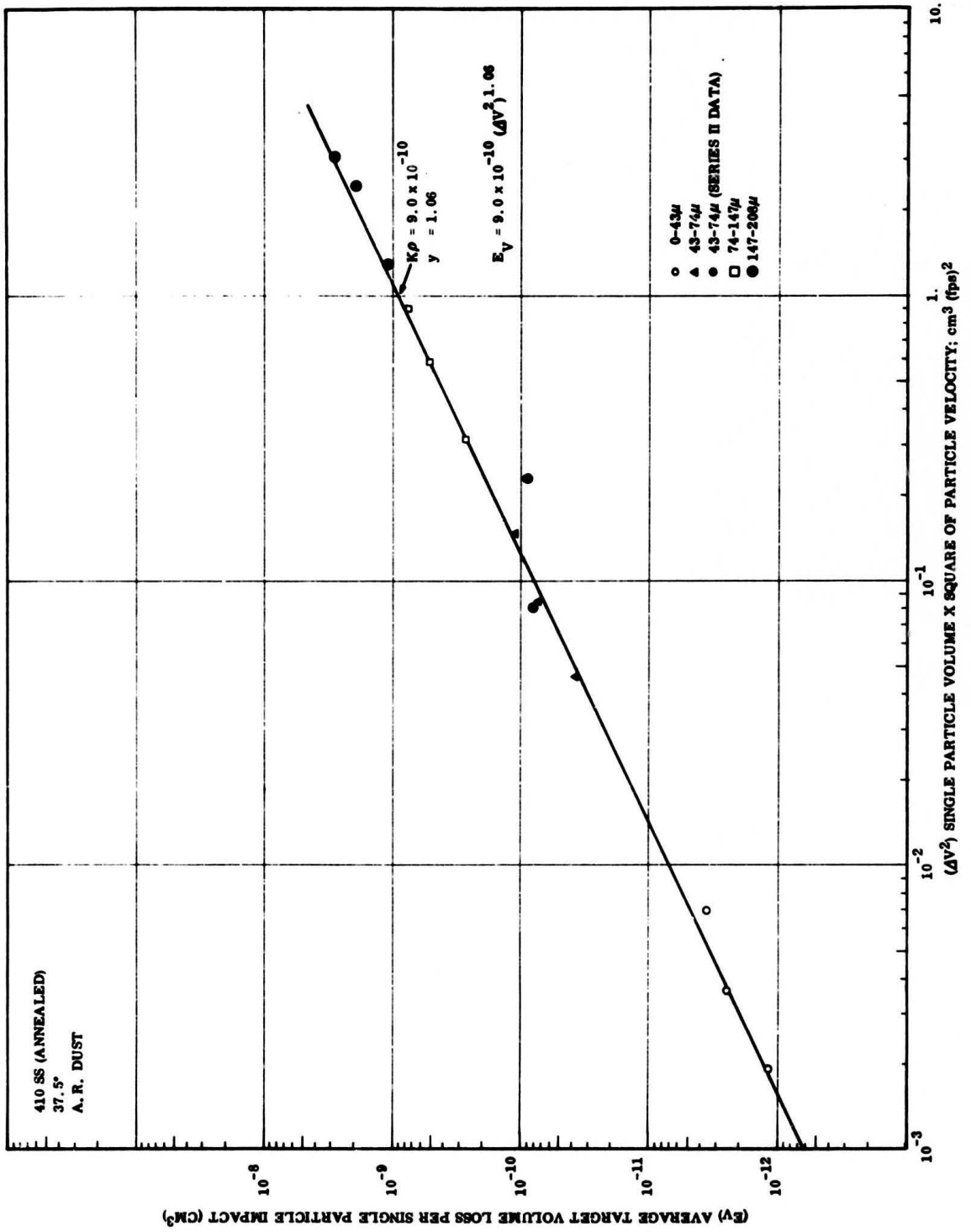


FIGURE 15. AVERAGE TARGET VOLUME LOSS PER SINGLE PARTICLE IMPACT
 (E_V) VERSUS ΔV^2

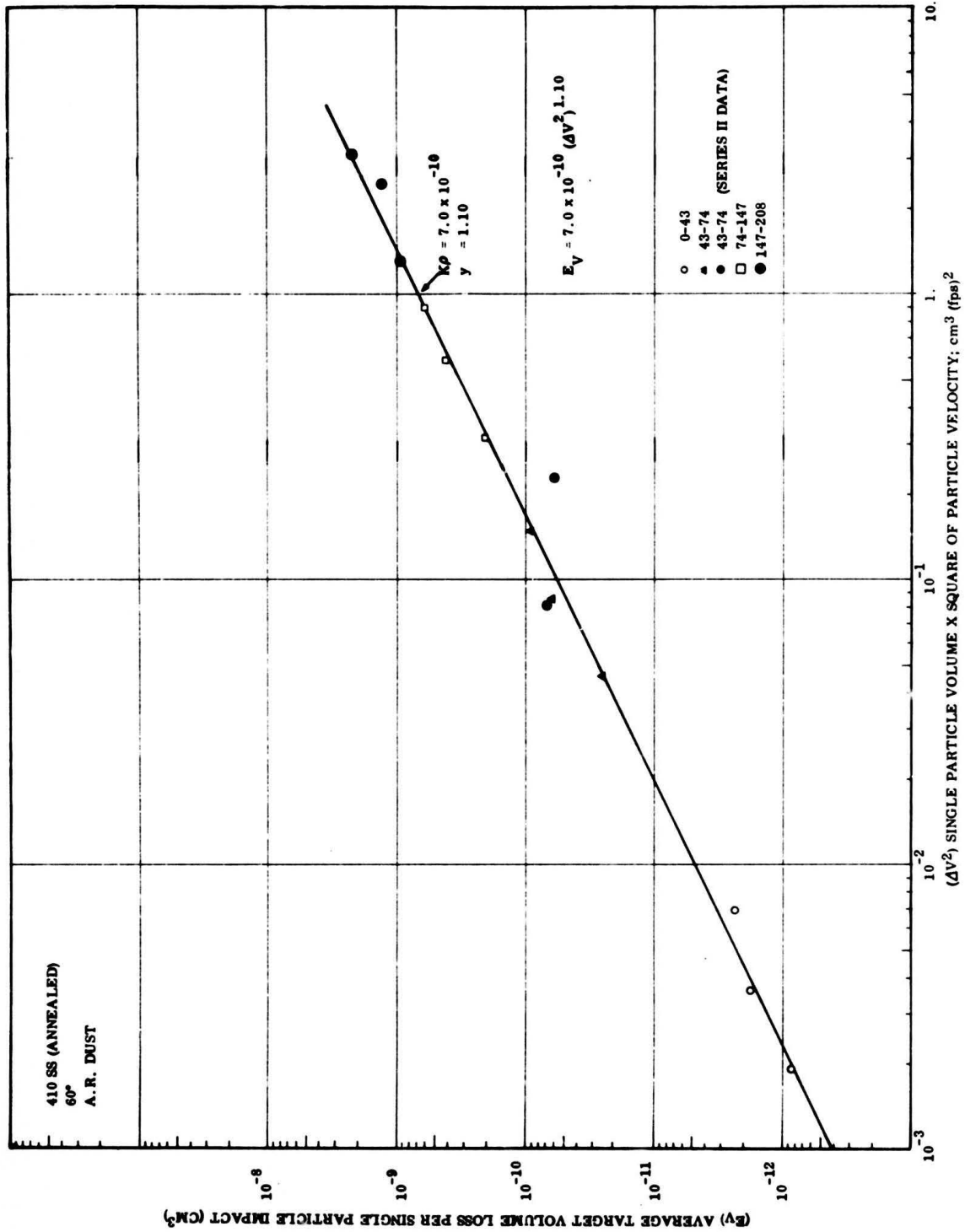


FIGURE 16. AVERAGE TARGET VOLUME LOSS PER SINGLE PARTICLE IMPACT
(E_V) VERSUS ΔV^2

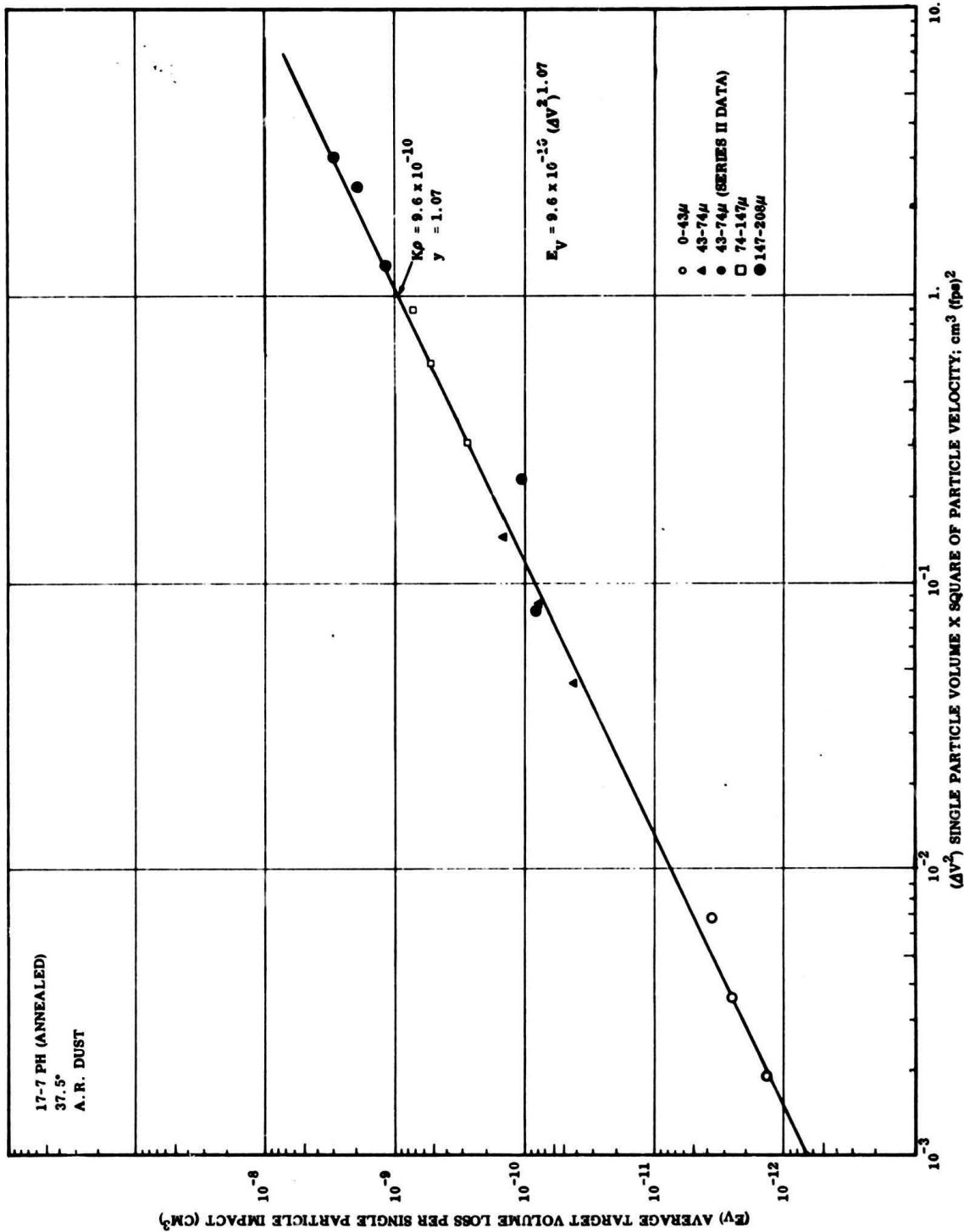


FIGURE 17. AVERAGE TARGET VOLUME LOSS PER SINGLE PARTICLE IMPACT
(E_V) VERSUS ΔV^2

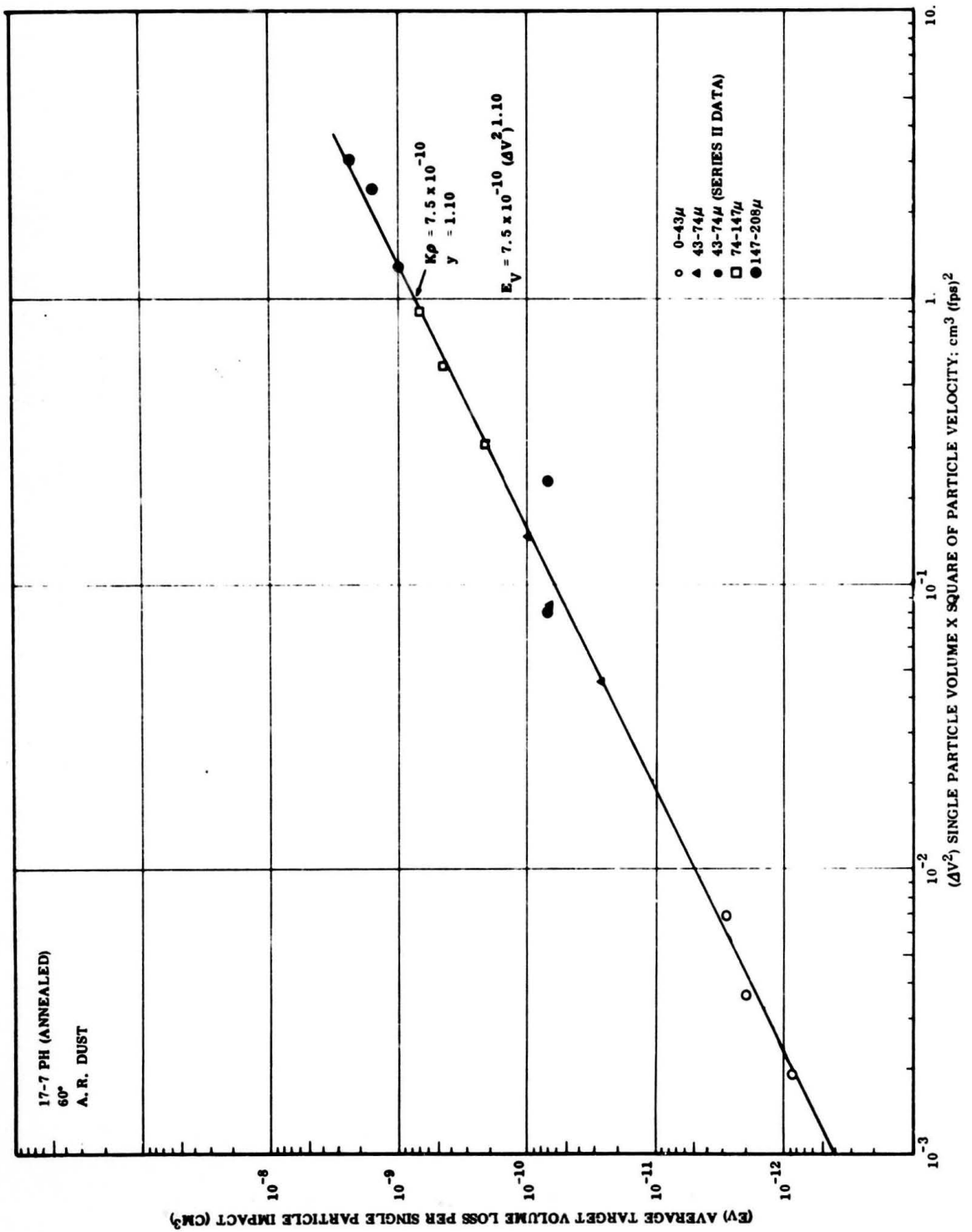


FIGURE 18. AVERAGE TARGET VOLUME LOSS PER SINGLE PARTICLE IMPACT (E_V) VERSUS ΔV^2

$$E_V = K\rho (\Delta V^2)^y \quad (4)$$

<u>Target Alloy</u>	<u>Impingement Angle (degrees)</u>	<u>$K\rho = \frac{C}{\Delta}$</u>	<u>y</u>
2024 Al	37.5	2.0×10^{-9}	1.04
	60	1.1×10^{-9}	1.00
Ti-6Al-4V	37.5	1.5×10^{-9}	0.99
	60	1.2×10^{-9}	1.08
410 SS	37.5	9.0×10^{-10}	1.06
	60	7.0×10^{-10}	1.10
17-7 PH	37.5	9.6×10^{-10}	1.07
	60	7.5×10^{-10}	1.10

The close similarity of the erosion responses for all targets is evident when all curves are plotted together (Fig. 19). The advantage in using all available data in a single plot to clarify relationships is well illustrated by these curves of E_V versus ΔV^2 . The correlations among the test variables expressed by equation (4) are sufficiently accurate to be made into nomographs relating Δ , V , and E_V . Figure 20 is a typical nomograph for the Ti-6Al-4V target (37.5° impingement angle).

It is apparent that erosion loss per particle is very nearly proportional to each particles' kinetic energy for all of the particle sizes (in the range of ~ 10 - 200μ), impingement angles (37.5 and 60°) and target alloys evaluated. This is remarkable, especially when considering that particle volume and mass range through 3 order of magnitude and particle energy through nearly 4 orders of magnitude. No evidence of an erosion threshold at the lower particle energies or particle sizes was discerned; so that even lower velocities and/or particle sizes will be necessary to study this phenomenon in future testing.

Data points from Series II work (43 - 74μ particle size) have been superimposed on the curves of E_V versus ΔV^2 (Fig. 11 through 18). Although all the Series II data conforms reasonably well to the curves, the lower velocity points tend to fall above the line, while the higher velocity points tend to fall below the line. This explains why the velocity exponents (x) calculated in Series II work all were less than 2.0 (Ref. 3).

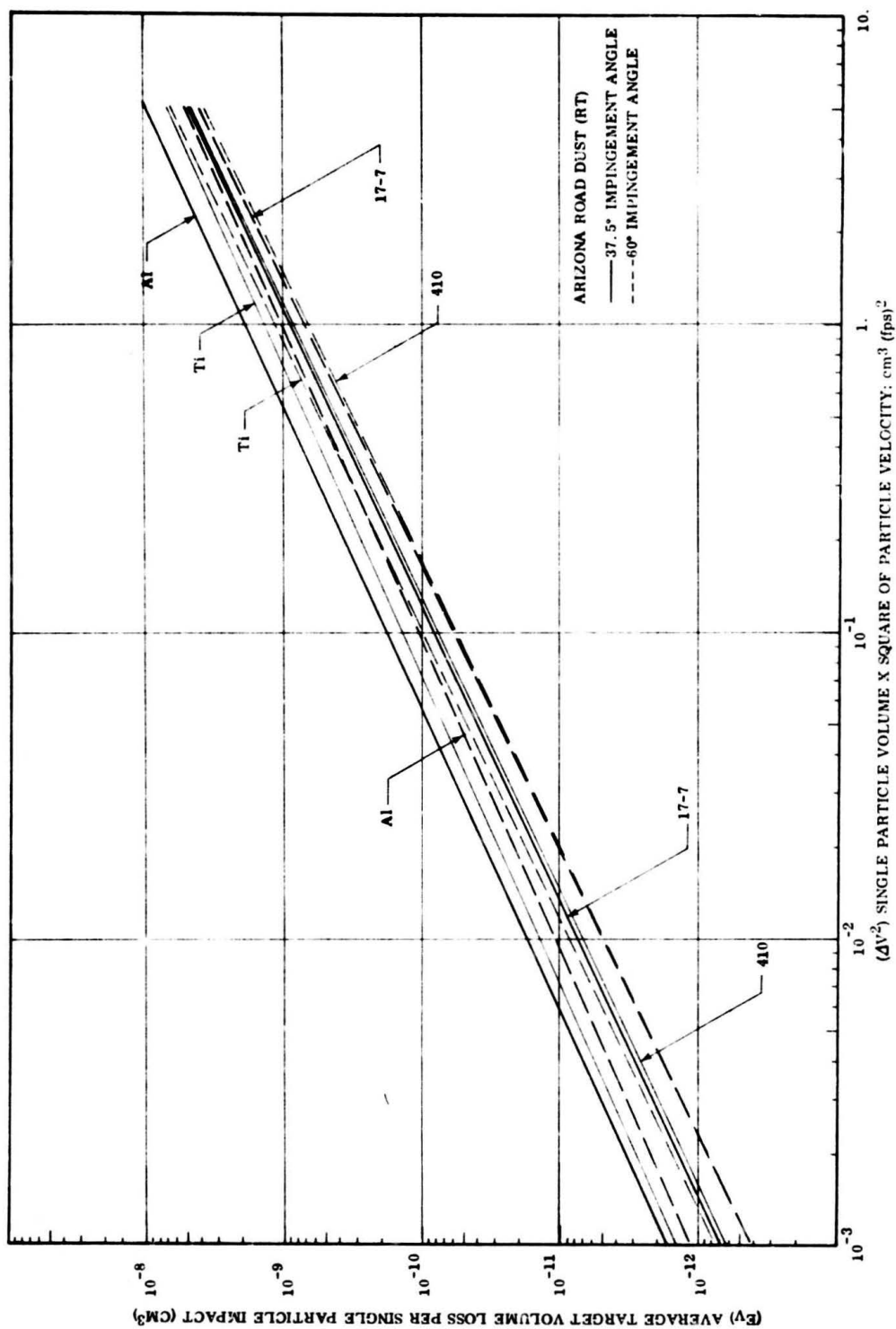
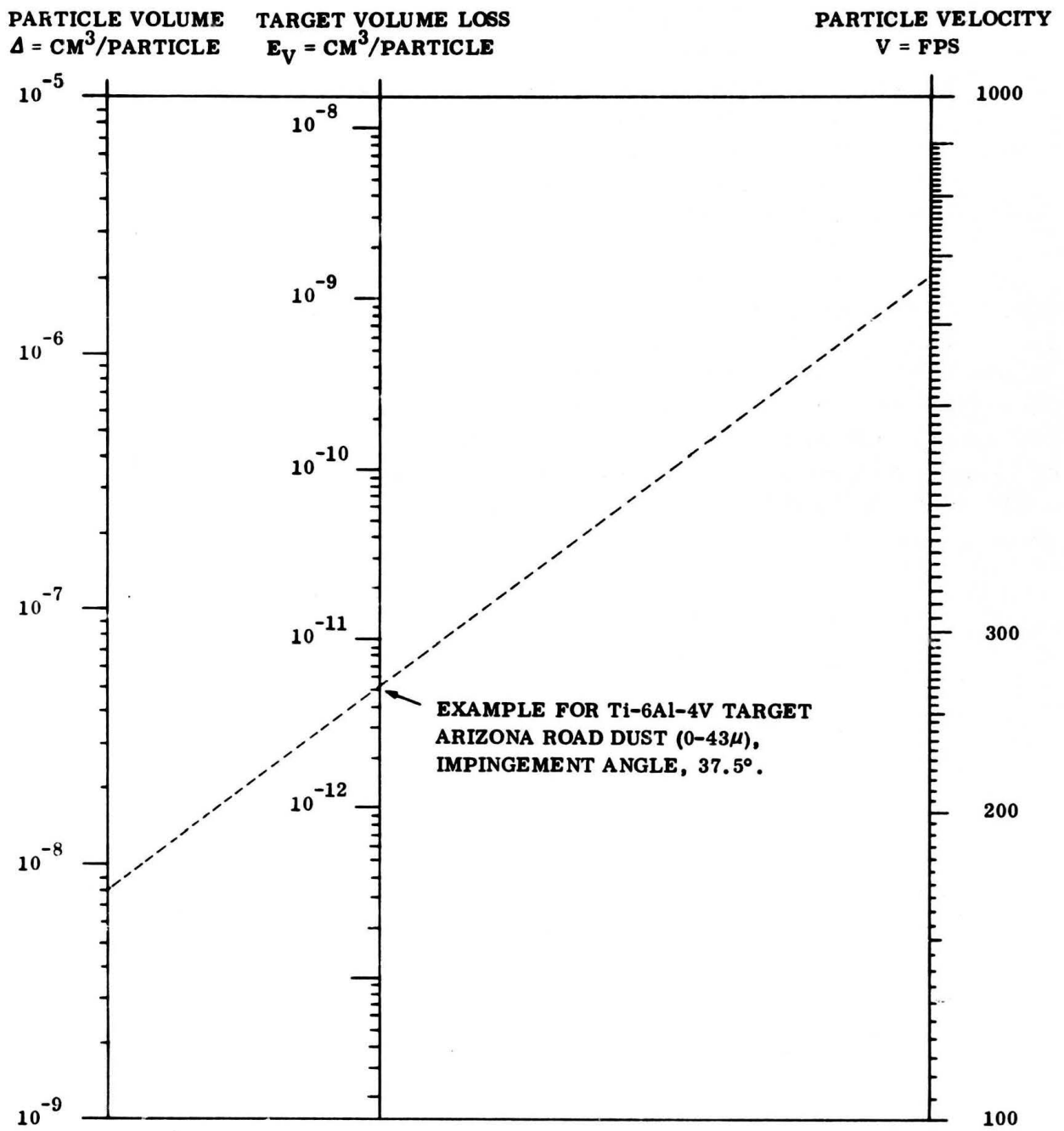


FIGURE 19. PLOTS OF E_V VERSUS ΔV^2 FOR ALL TARGET MATERIAL AND IMPINGEMENT ANGLE COMBINATIONS



**FIGURE 20. NOMOGRAPH RELATING Δ , V , AND E_V FOR THE Ti-6Al-4V TARGET
(A. R. DUST; 37.5° Impingement Angle)**

4.1.2 Test Format, Balance of Test Series III

Present plans call for a repeat of the Arizona Road Dust test schedule listed in Table I, with the test temperature raised to 700 F. In addition, the same schedules (RT and 700 F) will be repeated using Vietnamese laterite soil, classified into the same particle size fractions as the Arizona Road Dust. The objectives will be to determine what effects elevated temperature and a different dust variety have upon the relationships between erosion and particle mass and particle energy already developed for Arizona Road Dust at room temperature.

In order to obtain a better idea of just what visible features of the erosion surface relate directly to the erosion mechanism, a special set of erosion tests will be conducted to establish erosion thresholds for particle size, particle energy and particle shape. Possible changes or differences in erosion phenomena associated with the erosion thresholds will be detected by electron microscopic examination of surfaces subjected to 10,000 particle-impacts, after threshold levels for particle energy, size, and shape are established by standard erosion tests. A sales order has been placed for the following special varieties of silica (quartz) sand, which are required for this work -

Item	Mesh Size	Nominal Particle Size (μ)
Sharp, Pure Silica Sand (SiO_2)	3200	5
" " " " " "	1200	10
" " " " " "	800	20
" " " " " "	400	40
Pure Silica Glass (SiO_2)	800	20
(Rounded or Spherical Particles)	400	40

Work will commence with 20μ particles of sharp silica sand to search for an erosion threshold on the 410 stainless steel target material.

4.1.3 Preparation of Laterite Soil as Test Dust

Most natural-occurring dusts (e.g., Arizona Road Dust) owe their erosiveness to a high silica (SiO_2) content, usually ≥ 50 percent weight (Ref. 3). An apparent exception is the lateritic soil from Vietnam, which is reputed to be very damaging to helicopter turbines. A sample of laterite soil from Pleiku, Vietnam will be tested in

Series III to determine the influence of particle mass, size, and energy on erosion characteristics for a low-silica dust. The red-brown Pleiku soil has been analyzed, and it is comprised of 80-90 percent (vol.) clay minerals (principally hydrous oxides and silicates of aluminum and iron), with the balance predominantly quartz (SiO_2) and feldspars. The clay minerals of the laterite occur in the form of aggregate particles, $\sim 30\text{-}500\mu$, each aggregate made up of colloidal-size constituent particles. After decontamination for 24 hours at 400 F, samples of Pleiku laterite for Series III testing were readily classified by a dry sieving method at Solar into particle size fractions equivalent to those employed for the Arizona Road Dust classification, viz.,

<u>Particle Size Range</u>	<u>Sieve Sets</u>
-43μ	-325 mesh
$-74\mu/+43\mu$	-200 mesh/+325 mesh
$-147\mu/+74\mu$	-100 mesh/+200 mesh
$-208\mu/+147\mu$	- 65 mesh/+100 mesh

Even after oven baking at 400 F, the two finer fractions of laterite soil showed a marked tendency toward caking and bridging under light pressure, and were impossible to meter into the erosion tester using the Giannini powder feeder. Much better results were obtained using the new gravity feeder developed at Solar this quarter (Appendix B). Preliminary room-temperature erosion testing with the finest fraction (-43μ) has shown an interesting tendency for the laterite dust to stick to the target erosion surfaces, effectively protecting the targets from measurable erosion damage.

Density determinations made upon various fractions of Pleiku laterite resulted in very uniform densities, as might be expected for aggregates made up of common (colloidal) constituents. Curiously, the density for Pleiku laterite also proved similar to the reported density for Arizona Road Dust. A standard pycnometric method was employed.

<u>Fraction</u>	<u>Density (gm/cc)</u>
Pleiku laterite (0- 43μ)	2.39
Pleiku laterite (43- 74μ)	2.42
Pleiku laterite (74- 147μ)	2.44
Arizona Road Dust (Coarse)	2.41

4.1.4 Different Interpretations of the Dust Concentration Parameter

The concentration of dust in the carrier gas has been demonstrated as a significant factor in determining the efficiency of the erosion process (Ref. 1 and 2). The present method of reporting dust concentration, which has direct significance to the mechanism study, is in terms of the weight of dust (mgs) contained in a cubic foot of the compressed carrier gas at the nozzle exit. Thus, for a given dust variety and dust particle size, the spatial array or geometric concentration of dust particles (in terms of particles/ft³ or mg/ft³) and the effective inter-particle spacing or separation in the carrier-gas remains the same for constant dust concentration, regardless of differences in particle velocity and/or temperature (and corresponding changes in carrier-gas compression and density). Another kind of dust concentration; viz., the number of milligrams of dust or the number of dust particles striking a unit area of target surface normal to carrier-gas flow per unit time, is proportional to the reported dust concentration (in mgs./ft³ or particles/ft³) times the carrier-gas velocity (ft/sec) or the volume flow of carrier gas passing through the nozzle exit per unit time (ft³/sec). The current method of determining carrier-gas volume flow is to multiply mean carrier-gas velocity, measured with a pitot tube about 1/4 inch inside the nozzle throat, times the nozzle area. This volume flow is used to determine the metering rate for the test dust. The coefficient of discharge for the nozzle is assumed to be ≈ 1.00 , because the erosion profile (impression) on the target with the 1/4 inch nozzle indicates collimated flow (no divergence).

It is believed that the present method of reporting dust concentration will be most meaningful in the forthcoming Test Series IV, which is designed specifically to study the effect of dust concentration upon dust erosion and erosion mechanism. However, some thought is being given to possible methods for relating reported dust concentration in the carrier gas back to the corresponding concentration in the ambient air, prior to ingestion. This dust concentration in the ambient air, or air at standard temperature (T_1) and pressure, (P_1) has considerable engineering significance. An approximation of the marked increase in dust concentration due to carrier-gas compression in the turbine compressor can be obtained using the $PV = nRT$ relation (i.e.,

$$\frac{P_1 V_1}{T_1} = \frac{P_2 V_2}{T_2} .$$

However, an accurate estimate of carrier-gas static temperature (T_2) and static pressure (P_2), which are constantly changing in the acceleration nozzle due to friction losses and other effects, would be difficult, particularly at the nozzle exit. The consensus at Solar is that the most accurate conversion of reported dust concentration to a second temperature and pressure would derive from the pitot tube readings themselves. These readings can be related directly to mass (weight) flow of carrier gas as

well as to gas velocity (through empirically derived data charts), so that dust concentration could readily be reported in terms of mgs of dust per pound of carrier-gas. The weight of gas then could be converted to an equivalent volume at any desired static temperature and pressure. Calibration of the acceleration nozzle to obtain an accurate coefficient of discharge would be the only requirement.

V. SYNOPSIS OF PROGRAM STATUS

Experimental work on Test Series III (Task III) was started this period, and is one-third complete. The objective of Series III is to determine the effects of varying dust particle volume (Δ), mass (M), velocity (V), and kinetic energy ($\propto MV^2$ and ΔV^2) upon erosion losses. Plots of standard erosion factor (erosion loss per gram of dust impacted) versus dust particle volume (constant particle velocity) showed little variation in bulk erosion efficiency over the range of median particle size, 20μ - 178μ . A more definitive erosion parameter proved to be E_V , the average target volume loss per single particle impact. Plots of E_V versus particle volume (Δ) and the particle energy parameter (ΔV^2 , \propto particle kinetic energy) demonstrate that erosion loss per particle progresses systematically through about 3 orders of magnitude, while Δ and ΔV^2 vary similarly. When all of the data for each target alloy-impingement angle combination are considered together, the direct proportionality of erosion per particle (E_V) and particle energy (ΔV^2) is made readily apparent. However, within each particle-size division tested, wherein the particle energy parameter ranges through less than one order of magnitude, the velocity exponents vary unpredictably between 0 and +5. This situation is indicative that duplicate testing per data point (or triplicate testing as in Series II) is inadequate to define the particle velocity exponent accurately, when comparing individual data points for the same particle size. During the next period, the E_V versus ΔV^2 and E_V versus Δ curves will be utilized to determine possible thresholds of erosion at specific levels of particle volume and particle energy. Study of these erosion thresholds and the associated target surfaces by electron microscopy is expected to corroborate and amplify what is already known regarding erosion mechanisms.

Vietnamese laterite soil has been prepared as a test dust by classification into 4 particle size ranges, for direct comparison with the Arizona Road Dust. The effective density of the laterite agglomerates has been determined very similar to Arizona Road Dust (~ 2.4 gm/cc). Preliminary erosion testing with fine laterite dust has shown a marked tendency for the dust to form a thin but protective film on all target surfaces.

VI. REFERENCES

1. C. E. Smeltzer and W. A. Compton, "Mechanisms of Sand and Dust Erosion in Gas Turbine Engines", Quarterly Technical Progress Report No. 2 (1 October through 31 December 1968), conducted by Solar Division of International Harvester Co., San Diego, California under U. S. Army Contract DAAJ02-68-C-0056.
2. C. E. Smeltzer, M. E. Gulden, and W. A. Compton, "Mechanisms of Sand and Dust Erosion in Gas Turbine Engines", Quarterly Technical Progress Report No. 3 (1 January through 31 March 1969), conducted by Solar Division of International Harvester Co., San Diego, California under U. S. Army Contract DAAJ02-68-C-0056.
3. Wendy Sage, "The Erosive Characteristics of Natural Sands and Abrasive Dusts", N. G. T. E. Note No. NT 699, May 1969, National Gas Turbine Establishment, Pyestock, Hants, England.

APPENDIX A

TEST PLAN FORMAT

Test Series	Objectives	Principal Variables	Non-Varying Test Conditions		
			Blade Material (Target)	Carrier Air	Dust Suspension
I	Determine type of erosion response (ductile or brittle) and angle of maximum erosion for all candidate materials under average (baseline) erosion conditions.	<ul style="list-style-type: none"> (a) angle of incidence (α) (six levels; 10°, 20°, 30°, 45°, 60°, 90°) (b) Metallurgical Structure (two levels; heat treated for maximum strength and fully annealed for softest condition). <ul style="list-style-type: none"> a) 410 Stainless steel b) 17-7PH Steel c) Ti-6Al-4V Titanium Alloy d) 6066 or 2024 Aluminum Alloy e) Al-B or other suitable Composite <p>Comments: Total number of tests = 180.</p>	<ul style="list-style-type: none"> (a) Unstressed 	<ul style="list-style-type: none"> (a) Temperature: Room temperature (b) Velocity: 650 fps (c) Pressure: 1 atmosphere 	<ul style="list-style-type: none"> (a) Arizona Road Dust (fine) (43 to 74μ) (b) Concentration: 5 mg/ft^3
II	Determine influence of test temperature upon type of erosion response and erosion rate at maximum erosion angle. Investigate possibility of		<ul style="list-style-type: none"> (a) Test Temperature (four levels - Room Temperature, 200°F, 300°F and 400°F (Al alloys and composite)) 	<ul style="list-style-type: none"> (a) Unstressed (b) High-strength structure 	<ul style="list-style-type: none"> (a) Pressure: 1 atmosphere (b) Concentration: 5 mg/ft^3

TEST PLAN FORMAT

Test Series	Objectives	Principal Variables	Non-Varying Test Conditions		Dust Suspension
			Blade Material (Target)	Carrier Air	
	temperature/velocity interactions.	<ul style="list-style-type: none"> • Room temperature, 300°F, 500°F and 700°F (Ti alloy) • Room temperature, 400°F, 600°F and 800°F (SS). (b) Dust Velocity 650 ft/sec and 1100 ft/sec (c) Angle of incidence (α) (three levels; maximum angle in previous tests plus two others to define response) <p>Comments: Total number of tests = 360</p>			<ul style="list-style-type: none"> (a) Concentration; 5 mg/ft³ (b) Angle of incidence for maximum erosion
III	Establish the effect upon erosion rate and mechanism of the dust energy factor (MVF ²) at critical (probably terminal) test temperatures. Incorporate different sizes and species of dust particles. Determine singular effects of particle velocity, particle energy,	<ul style="list-style-type: none"> (a) Velocity (four levels, between 500 fps and 1500 fps) (b) Dust species (two types, Arizona Road Dust and Laterite) (c) Particle Sizes (four levels) <ul style="list-style-type: none"> • 0 to 43μ • 43 to 74μ 	<ul style="list-style-type: none"> (a) All materials unstressed. (b) High-strength structure 	<ul style="list-style-type: none"> (a) Pressure, 1. atmosphere 	<ul style="list-style-type: none"> (a) Concentration; 5 mg/ft³ (b) Angle of incidence for maximum erosion

TEST PLAN FORMAT

Test Series	Objectives	Principal Variables	Non-Varying Test Conditions		
			Blade Material (Target)	Carrier Air	Dust Suspension
	particle size and mass as well as interactions of these variables in combination.	<ul style="list-style-type: none"> • 74 to 148μ • 148 to 210μ (d) Test temperature (two levels, room temperature and maximum service temperature) 			
					<p>Comments: Total number of tests = 960</p> <p>Important interactions to be studied:</p> <ul style="list-style-type: none"> • Velocity/mass • Velocity/size • Velocity/temperature • Temperature/mass • Velocity/temperature/mass • Velocity/dust species
IV	Assess (universal) validity of erosion factor (e) remaining constant within normal range of dust concentrations (Montgomery and Clark). Determine reason for erosion	<p>(a) Dust Concentrations: (five levels)</p> <ul style="list-style-type: none"> • 5 mg/ft³ • 10 mg/ft³ • 20 mg/ft³ • 30 mg/ft³ • 40 mg/ft³ 	<p>(a) All materials unstressed.</p> <p>(b) High-strength structure.</p>	<p>(a) Pressure, 1. atmosphere</p>	<p>(a) Angle of incidence for maximum erosion.</p>

TEST PLAN FORMAT

Test Series	Objectives	Principal Variables	Non-Varying Test Conditions		
			Blade Material (Target)	Carrier Air	Dust Suspension
	factor dependency upon dust particle size. [e = grams, blade weight loss/grams, dust ingested]	(b) Particle sizes (two levels, based upon preceding tests) (c) Dust species (two types, Arizona Road Dust and Laterite) (d) Test temperature (two levels, based upon preceding tests) (e) Dust velocity (two levels, based upon preceding tests)			

Comments: Total number of tests = 1200

Important interactions to be evaluated:

- Concentration/velocity
- Concentration/velocity/Temp.
- Concentration/mass or Concentration/Size
- Concentration/Temperature

TEST PLAN FORMAT

Test Series	Objectives	Principal Variables	Non-Varying Test Conditions		
			Blade Material (Target)	Carrier Air	Dust Suspension
V	• Concentration/Temperature/Species [Using data from series (2), (3) and (4) testing.]	Determine modification of erosion behavior by loading specimen in tension to various percentages of the design or flow stress (design stress \approx 60% of the 0.2% yield strength at service temperature)	(a) Imposed Stress (three levels - • 20% of yield strength • 40% of yield strength • 60% of yield strength) (b) Test temperature two levels (to be determined). (c) Dust velocity two levels (to be determined) (d) Dust species (two types, Arizona Road Dust and Laterite)	(a) High-strength structure (b) All materials.	(a) Angle of incidence for maximum erosion. (b) Concentration: 5 to 20 mg/ft ³ (c) Particle size range 43 to 74 μ
VI	Total number of tests = 360.	Evaluate importance of carrier gas pressure as a variable influencing erosion.	(a) Carrier gas pressure (two levels) 2 and 4 atmosphere (Al alloy and	(a) High-strength structure	(a) Angle of incidence for maximum erosion

TEST PLAN FORMAT

Test Series	Objectives	Principal Variables	Non-Varying Test Conditions		
			Blade Material (Target)	Carrier Air	Dust Suspension
		composite) 5 and 10 atmosphere (Ti alloy) 8 and 16 atmosphere (SS) (b) Test temperature (two levels) (c) Dust velocity (two levels) (d) Dust species (two types, Arizona Road Dust and Laterite)	(b) All material un-stressed.		(b) Concentration: 5-20 mg/ft ³ (c) Particle size range 43 to 74 μ
					Total number of tests = 240
					GRAND TOTAL OF TESTS = 3300

APPENDIX B

DESIGN AND OPERATION OF NEW GRAVITY-FEED DUST METER

Fine test dusts have a disturbing tendency to cake together and clog the feeder orifice of rotary-type dust feeders, preventing uniform dust metering and often-times stopping flow altogether. Inasmuch as a wide variety of dust sizes and types are required on the subject program, it was desired to have a single dust feeder available with sufficient flexibility to meter all test dusts uniformly. The Gianinni rotary-type feeder proved incapable of handling the $0-43\mu$ size powders (both Arizona Road Dust and Vietnamese laterite). Consequently, a simple gravity-type feeder was devised at Solar with an adjustable oscillating plunger to provide the necessary agitation of the dust feeding into the orifice to eliminate caking and clogging problems. A schematic diagram of the new feeder showing the relationship of the orifice and the mating plunger is illustrated in Figure B-1. The plunger is activated by a variable-speed, electric-motor controlled cam. The orifice opening (clearance) can be controlled between 0-1/8 inch by adjusting the length of the plunger rod. The rate of plunger oscillation can be controlled continuously between 20-200 cycles per minute.

To ensure a uniform feeding rate during actual erosion testing, preliminary metering runs are made with the prescribed size, type, and charge weight of test dust, to collect and weigh the quantities of dust metered out each minute of a simulated test run. The cam speeds and plunger-orifice clearances are varied experimentally during each run until a uniform metering rate is obtained. A distinct advantage of the new meter is that the quantity of test dust is pre-weighed for each test, eliminating possible error in the amount of dust ingested from test-to-test.

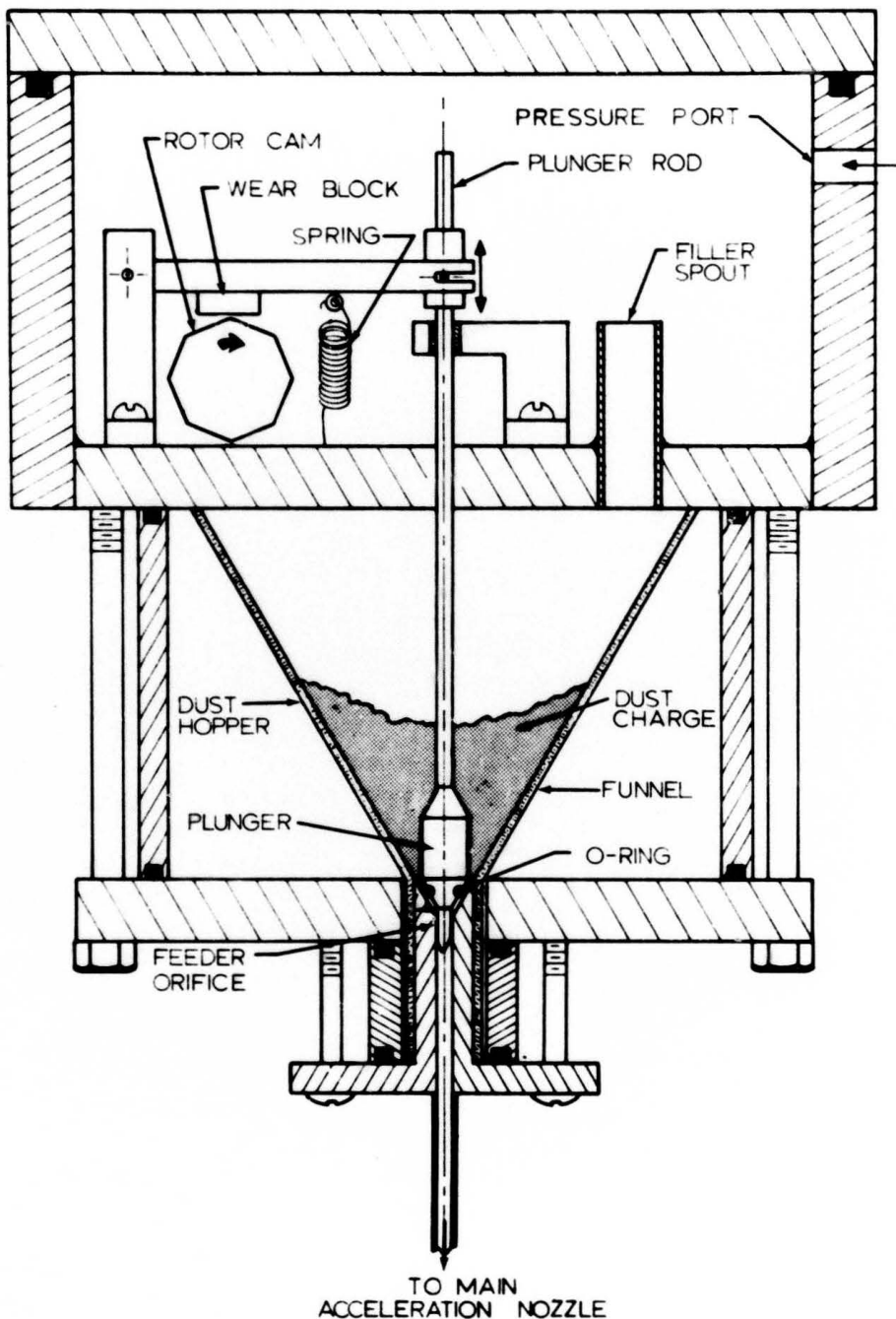


FIGURE B-1. SKETCH OF GRAVITY-FEED POWDER METER